Chemical Diversification of Angucycline Natural Products: Heterologous Expression of Lugdunomycin Tailoring Genes

Master's thesis

Department of Life Technologies
Cell Biology

18.8.2025

Turku

Sofia Antin

The originality of this thesis has been checked in accordance with the University of Turku quality assurance system using the Turnitin Originality Check service.

UNIVERSITY OF TURKU
Department of Life Technologies
ANTIN, SOFIA: Chemical Diversification of Angucycline Natural Products: Heterologous Expression of Lugdunomycin Tailoring Genes

Pro gradu thesis, 75 p.
Molecular Biosciences, Cell Biology

August 2025

Antimicrobial resistance is a quickly growing threat with a huge global impact. Majority of antibiotics have been sourced from soil-dwelling *Streptomyces* bacteria, which are naturally tremendous at producing broad-spectrum antibiotics, such as kanamycin and streptomycin. Still, their potential as antimicrobial compound producing organisms is to be fully harnessed. According to genomic mining studies, *Streptomyces* is known to have the ability to produce numerous unknown secondary metabolites with potential bioactivity.

Polyketides are the largest group of secondary metabolites produced by *Streptomyces*. Several polyketides, such as tetracycline and erythromycin, are in wide clinical use as, for example, antibacterials, antitumor agents, and antifungals. Angucyclines are a large and diverse group of aromatic polyketides distinguished by their unique bent four-ring benz[*a*]anthraquinone scaffold. Lugdunomycin is an angucycline-derived secondary metabolite. It has gained great interest due to its unique structure and elusive biosynthetic pathway. Lugdunomycin represents a novel subclass of aromatic polyketides that have undergone cleavage of the C-ring, leading to drastic and complex structural arrangements.

The lugdunomycin pathway is still to be fully characterized, as the biosynthesis requires multiple complex steps. The aim of this study was to construct the pathway step by step using the BioBricks method for heterologous expression in *Streptomyces*. Thus, a library consisting of single gene building blocks could be established. Producing the pathway intermediates for enzymatic assays provides essential information about the mechanism of the biosynthesis. Understanding the pathway is of great importance as it would greatly benefit designing novel synthetic antibiotic structures.

Keywords: antibiotic, *Streptomyces*, polyketides, angucyclines, lugdunomycin

Table of contents

Abbreviations

ACP	Acyl carrier protein
AMR	Antimicrobial resistance
ARO	Aromatase
ABM	Antibiotic biosynthesis monooxygenase
AT	Acyl transferase
BGC	Biosynthetic gene cluster
CoA	Coenzyme A
CYC	Cyclase
DBTL	Design-build-test-learn
DH	Dehydratase
EDTA	Ethylenediaminetetraacetic acid
ER	Enoylreductase
FAD	Flavin adenine dinucleotide
KR	Ketoreductase
KS	Ketosynthase
LB	Luria-Bertani
minPKS	Minimal polyketide synthase
MS	Mannitol soy flour
NADPH	Nicotinamide adenine dinucleotide phosphate
PKS	Poyketide synthase
R2YE	Rich medium 2 with yeast extract
RBS	Ribosome binding site
SDS	Sodium dodecyl sulfate
SG	Soytone glucose
TAE	Tris-acetate-EDTA
TE	Thioesterase
TE	Tris-EDTA
Tris	Tris(hydroxymethyl)aminomethane
TSB	Tryptone soy broth
UHPLC	Ultra-high performance liquid chromatography
UV-Vis	Ultraviolet and visible light
YEME	Yest extract malt extract
YT	Yeast extract-tryptone

1 Introduction

Antimicrobial resistance (AMR) is a rapidly growing threat with a huge global impact. In a 2013 G8 summit, AMR was identified as the "major health security challenge of the 21st century" (G8 Science Ministers 2013). The overuse and misuse of antibiotics in humans, agriculture, animal farming, and industry have been the main drivers of AMR during the past 80 years, which has led to a remarkable increase in its prevalence in the last decades (Christaki et al. 2020; European Centre for Disease Prevention and Control. 2018). In addition, globalization has facilitated the spread of resistant organisms further than ever before, introducing local microbial populations to foreign resistance mechanisms (Morrison and Zembower 2020). This has contributed to the emergence of "superbugs" and multidrug-resistant bacterial strains, such as multidrug-resistant *Acitenobacter baumannii*, *Klebsiella pneumoniae*, and methicillin-resistant *Staphylococcus aureus* (MRSA) along with several others, therefore giving rise to a previously unseen major global health threat (Christaki et al. 2020).

In 2024, the World Health Organization estimated that bacterial AMR was directly responsible for 1.27 million global deaths in 2019, as well as contributing to 4.95 million. In addition to causing death and disability, AMR leads to significant economic consequences, generating to up to US$ 1 trillion additional healthcare costs by 2050, according to The World Bank estimates. The impact of AMR is seen across all regions and income levels, although low- and middle-income countries are most severely affected. (World Health Organization 2024) As antibiotics form the cornerstone of modern medicine, the continued rise of resistance threatens to undermine decades worth of medical progress.

A crucial and urgent need for new antimicrobial drugs has arisen during the past decades, especially for newer classes unaffected by known resistance mechanisms. (Bush et al. 2011). Unfortunately, however, the current low development pace of therapeutics with a novel mode of action does not even closely correspond to the pace in which AMR is developing. Moreover, the therapeutics targeting WHO priority pathogens currently in clinical trials do not contain advanced mode of action but are rather derivatives of existing classes of antibiotics. (Beyer and Paulin 2020) During the past 40 years, only a small fraction of antibiotics approved for treatment represented new compound classes. The poor development rate of novel therapeutics is partially due to the lack of research and

tools and methodologies facilitating antibiotic discovery. (Miethke et al. 2021) In addition, although the antibiotic crisis is widely acknowledged, several factors, including economic, regulatory, and societal aspects contribute to the declining rate in which antibiotics are being discovered and developed (Årdal et al. 2020).

Of the antibiotics in clinical use today, more than three quarters are natural products produced by organisms including bacteria and fungi or semi-synthetic derivatives of such naturally produced compounds (Durand et al. 2019). Difficulties in culturing and producing new compounds in laboratory conditions has long been an issue due to several genes remaining unexpressed, thus resulting in a decline of discovery of new compounds. The decline is, however, not due to exhaustion of the biosynthetic gene resources but rather due to the limited methods in microbial isolation, cultivation, and bioactivity screening (Li et al. 2018). For example, modifications to the culture conditions, studying bacterial hormones, and mimicking the natural environment of bacteria through co-culturing, are used to enhance antibiotic production (Antoraz et al. 2015). In addition, to yield the previously unexpressed secondary metabolites, the research is now shifting towards modern engineering techniques such as genome mining and biosynthetic engineering. (Lacey and Rutledge 2022; Miethke et al. 2021) Genome mining refers to investigations into the biosynthetic pathways and the chemical structure of natural products using bioinformatic methods. This often results in the discovery of previously uncharacterized natural product biosynthetic gene clusters (BGC), that can be systematically expressed in specialized heterologous hosts. (Albarano et al. 2020; Miethke et al. 2021)

1.1 *Streptomyces* as producers of natural compounds

Streptomyces is a large genus of Gram-positive, soil-dwelling *Actinobacteria* characterized by their diverse strains, complex secondary metabolism, and complex developmental life cycle (Komaki 2023). They grow as filamentous mycelia and form aerial hyphae and spores as a response to environmental cues. This developmental progression is closely linked to the production of natural products, which often serve specific physiological or ecological functions. (Jones and Elliot 2017). These compounds carry a great chemical diversity and have been harnessed early on for treatment of human diseases either directly, or later as synthetic or semi-synthetic derivatives. Today, a wide range of natural products are produced industrially from microorganisms, with

Streptomyces emerging as one of the most notable sources. Among the various classes of clinically used compounds originating from *Streptomyces*, antibiotics have arguably been the most significant. Actinomycetes account for approximately 80 % of the sources of antibiotics in current clinical use, with *Streptomyces* being the major contributor (De Lima Procópio et al. 2012). Some of the most significant *Streptomyces*-derived antibiotics include tetracycline, streptomycin, and chloramphenicol. (Watve et al. 2001). However, the potential of *Streptomyces* as antimicrobial compound producing organisms is to be fully harnessed (Baltz 2016). Studies suggest that the *Streptomyces* genus might be able to produce around 150,000 more bioactive compounds than all *Streptomyces* secondary metabolites reported today (Lacey and Rutledge 2022). Since the golden era of antibiotic discovery in 1950s, the finding of new compounds has slowed down tremendously, while several resistant bacterial strains have arisen. There is an urgent, ever-growing need for novel antimicrobial compounds, as well as for new methods to discover and characterize these compounds. For these reasons, the unharnessed potential of *Streptomyces* may become a key factor in solving the AMR emergency. (Van Der Meij et al. 2017)

The whole-genome sequencing of several *Streptomyces* sp. has revealed an abundance of biosynthetic gene clusters that remain unexpressed when cultivated in standard laboratory conditions (Aigle et al. 2014). Moreover, there are likely many actinomycetes yet to be discovered and characterized (Zhang et al. 2024). This highlights the great potential these organisms still carry in finding new bioactive molecules, including likely previously unseen classes of secondary metabolites. As a result of these findings, the strategies in finding new compounds have shifted from traditional high-throughput bioactivity screenings to more multidisciplinary approaches. These include genome mining, bioengineering of biosynthetic gene clusters, and omics-based tools (Genilloud 2019) Activation of unexpressed, cryptic biosynthetic gene clusters encoding unknown metabolites has long been a bottleneck with the traditional approaches. These are gene clusters present in microbial genomes that encode potential natural products but remain silent or unexpressed, so their metabolites are unknown (Nguyen et al. 2020). The newer strategies provide prominent methods that involve activating these gene clusters through techniques such as heterologous expression, which involves transferring the gene cluster in a different, more easily manipulated host organism. Modern methods in genome engineering and synthetic biology have recently facilitated this approach thus exposing untapped areas in the chemical diversity of natural products. (Baltz 2016)

Besides enabling the discovery of novel compounds, the study of biosynthetic pathways in *Streptomyces* deepens our understanding of the whole underlying metabolic networks. The discovery of novel antimicrobials and other bioactive compounds through genome screenings has gained a growing interest. Combined with traditional biological screening, the usage of genome-mining tools could greatly enhance the discovery of novel antimicrobial and other bioactive compounds. (Cibichakravarthy and Jose 2021) Although the individual genes and proteins involved in *Streptomyces* secondary metabolism are highly diverse and strain-specific, the pathways do share conserved elements in enzyme structure, regulation, and biosynthetic logic, common to both primary and secondary metabolism (Smith and Tsai 2007). Genetic similarity network analyses allow the application of research findings to related pathways, thereby accelerating their characterization and engineering through network modelling. Many of the enzymes involved have conserved homologs across *Streptomyces* strains and species, and elucidating the structure and function of one enzyme can help identify homologs through comparative genomics. (Navarro-Muñoz et al. 2020) Therefore, each characterized *Streptomyces* metabolic pathway can be considered as reference guiding future research by helping discover related pathways and genes, as well as to help focus on the most promising gene clusters. This helps to cleave a path towards more efficient natural product research.

1.2 Polyketides

Polyketides are a highly diverse group of secondary metabolites produced by microorganisms including *Streptomyces*. Several polyketides, such as tetracycline, erythromycin, and doxorubicin, are in wide clinical use as, for example, antibacterials, antitumor agents, and antifungals in the treatment of various diseases (Jia Wang et al. 2020). Polyketides have also recently become a major interest in synthetic biology research. Novel polyketides are produced by engineering the polyketide-producing biosynthetic pathways, and known polyketides are optimized for improved therapeutic properties (Malico et al. 2020). Despite being synthesized from structurally simple building blocks, they exhibit a remarkable structural diversity that determines the diverse biological functions they carry.

Polyketides are synthesized in complex biosynthesis pathways by a family of enzymes known as polyketide synthases (PKS), which are classified into three types based on their

structure and specific reaction mechanisms. (Risdian et al. 2019). Type II polyketide synthases are responsible for the production of many clinically relevant, especially aromatic compounds with great structural diversity, such as tetracyclines and doxorubicin (Rivers and Lowell 2024). The process is analogous with fatty acid synthesis, with both using a common pool of simple carbon precursors that are extended in highly organized, repetitive reactions to form long carbon chains (Hertweck 2009). The type II polyketides act iteratively to catalyze the protein-tethered polyketide chain elongation and further modifications via multiple cooperatively acting monofunctional enzymes. Alternatively, the type I enzymes contain huge multifunctional proteins with each domain acting only once in an assembly line fashion, and whereas type III enzymes act as simpler stand-alone ketosynthases accepting CoA-based substrates without a carrier protein (Xie and Zhang 2023). The types also differ in the organisms in which they are found (Nivina et al. 2019).

The type II polyketide synthase consists of a core set of multifunctional enzymes referred to as the minimal polyketide synthase (minPKS), which is responsible for constructing the initial polyketide scaffold. The minPKS consists of enzymes responsible for the carbon chain elongation by a ketosynthase, chain length factor, and a carrier protein. (Xie and Zhang 2023) The ketosynthase (KS) heterodimer consists of two subunits, ketosynthase alpha (KSα), and a chain length factor (KSβ/CLF). Together they catalyze an iterative decarboxylative condensation reaction, in which two-carbon extender units, usually malonyl coenzyme A (malonyl-CoA), are attached to a starter unit, usually acetyl coenzyme A (acetyl CoA). The extender units are loaded onto acyl carrier proteins (ACP) forming acyl-ACP, and acetyltransferase (AT) facilitates their transfer. The ACP-bound extender unit reacts with the upstream polyketide of a growing polyketide chain by undergoing a decarboxylative Claisen condensation reaction catalyzed by the KS complex. Chain length is determined by the CLF subunit of ketosynthase, and the release of the polyketide chain is catalyzed by a thioesterase (TE) domain. (Hertweck et al. 2007; Malico et al. 2020; Risdian et al. 2019) The resulting polyketide chain is very unstable and will quickly be converted into various end products with post-PKS tailoring (Rivers and Lowell 2024). The enzyme complex with the initial carbon scaffold is described in figure 1.

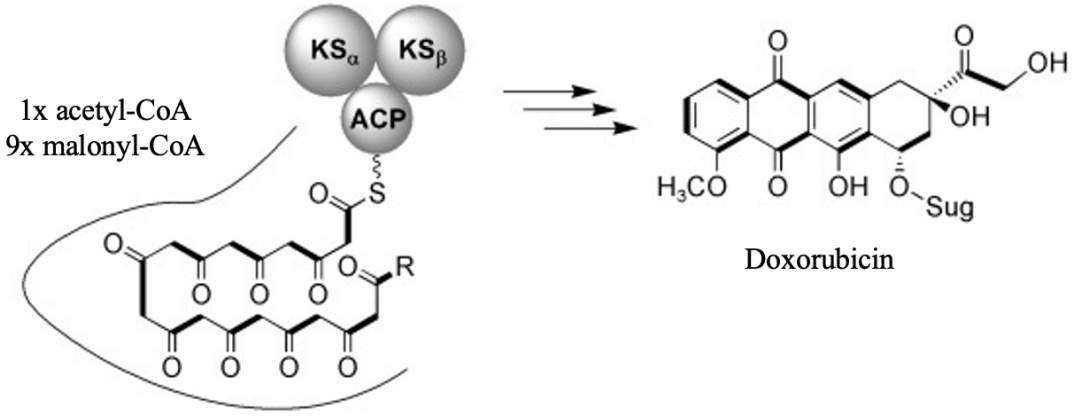

Figure 1. Type II polyketide synthase (PKS). A type II PKS features two ketosynthase (KS) subunits α and β that catalyze an iterative reaction in which malonyl-CoA extender units bound to an acyl carrier protein (ACP) are repeatedly added to an acetyl-CoA starter unit. The reaction yields a long carbon-chain intermediate that will undergo further tailoring modifications to yield rearranged polycyclic polyketides, such as doxorubicin. Figure modified from Hertweck et al. 2007.

The great chemical diversity that characterizes polyketides arises from the action of post-PKS tailoring enzymes, that modify the initial carbon frame into various directions by rearranging the scaffold and introducing different molecules and functional groups. These modifications include the cyclization of the polyketide chain via cyclases (CYC) and aromatases (ARO). (Rivers and Lowell 2024) The remaining structure can contain, for example, linear or angular aromatic structures, fused aromatic ring structures, and cleaved rings. Several atoms and groups can be introduced via hydroxylation, methylation and oxygenation. Some compounds contain sugar moieties introduced by glycosyltransferases (GT) in glycosylation. Acyltransferases (AT) catalyze the attachment of acyl chains of varying lengths to amine and alcohol moieties. Reductases, such as ketoreductases (KR), convert ketones to secondary alcohols, and dehydrogenases transfer electrons and protons to the substrate. There are also halogenating enzymes, that introduce, for example, chloride and bromide atoms to carbons, therefore greatly influencing the biological activity of the molecule. (Olano et al. 2010) There has been a growing interest in engineering native post-PKS enzymes to diversify the bioactive compound selection further by creating even more complex structures with enhanced functionality (Malico et al. 2020).

1.3 Angucyclines

Angucyclines are a large and diverse group of polyaromatic polyketides produced by type II polyketide synthases in microorganisms. Both marine and terrestrial actinomycetes, most importantly *Streptomyces*, are a significant source of angucyclines (H.-S. Liu et al. 2025; Vysloužilová and Kováč 2024). Angucyclines and their derivatives have shown to carry both anticancer and antimicrobial properties, which has led to a broad interest and research in the hope of gaining new antibiotic agents and other bioactive compounds for clinical use. They exhibit a huge chemical diversity due to modifications in the carbon scaffold itself or the attachment of various substituents. The diverse biological functions that yield from the unique and versatile structures have made angucyclines a great target in drug discovery. (H.-S. Liu et al. 2025)

Over 300 types of angucyclines and angucyclinones have been isolated since the first one in 1965. However, none of them are in clinical use today. (Vysloužilová and Kováč 2024) This is largely due to toxicity and solubility issues (Kharel, Pahari, Shepherd, et al. 2012), or low amount of material isolated from natural sources, as these compounds are often produced only in trace amounts (Vysloužilová and Kováč 2024). Moreover, many angucyclines are encoded in silent biosynthetic gene clusters that are poorly expressed (Palmu et al. 2007). As secondary metabolites, they are commonly expressed only as a response to specific signals or stressors, and understanding the regulatory genes mediating the secondary metabolism is difficult in laboratory conditions (Bibb 2005). Additionally, the complex molecular architecture makes the synthesis of these compounds challenging. The *in vivo* biosynthesis of these compounds is branched out into an extremely complex network with several by-products and shunt pathways (Patrikainen et al. 2012). However, improved understanding of metabolic networks and advanced strain and genome engineering tools have made it possible to produce and study various previously undisclosed compounds. This highlights the great potential there still is in making novel discoveries within these metabolic networks in effort to address the growing challenges AMR is posing. (Bibb 2005; Yook et al. 2025)

Many angucycline biosynthesis pathways are well-known and studied and follow a pathway of typical aromatic polyketides. The biosynthesis begins with ten acetate building blocks. A type II PKS synthesizes the initial structure forming a linear decaketide by repeated condensation reactions between an acetyl-CoA starter unit and nine malonyl-

CoA extender units. The unstable linear decaketide intermediate formed by minPKS is immediately reduced by a ketoreductase, and the tetracyclic structure is established by an aromatase and a cyclase as shown in figure 2. (Hertweck et al. 2007; Palmu et al. 2007) The first stable intermediates and key products in all angucycline pathways are UWM6 and 2,3-dehydrorabelomycin, which is also known as prejadomycin. The formation of these intermediates is followed by various modification steps catalyzed by post-PKS tailoring enzymes that are responsible for the great chemical diversity across angucyclines. (Fan and Zhang 2018).

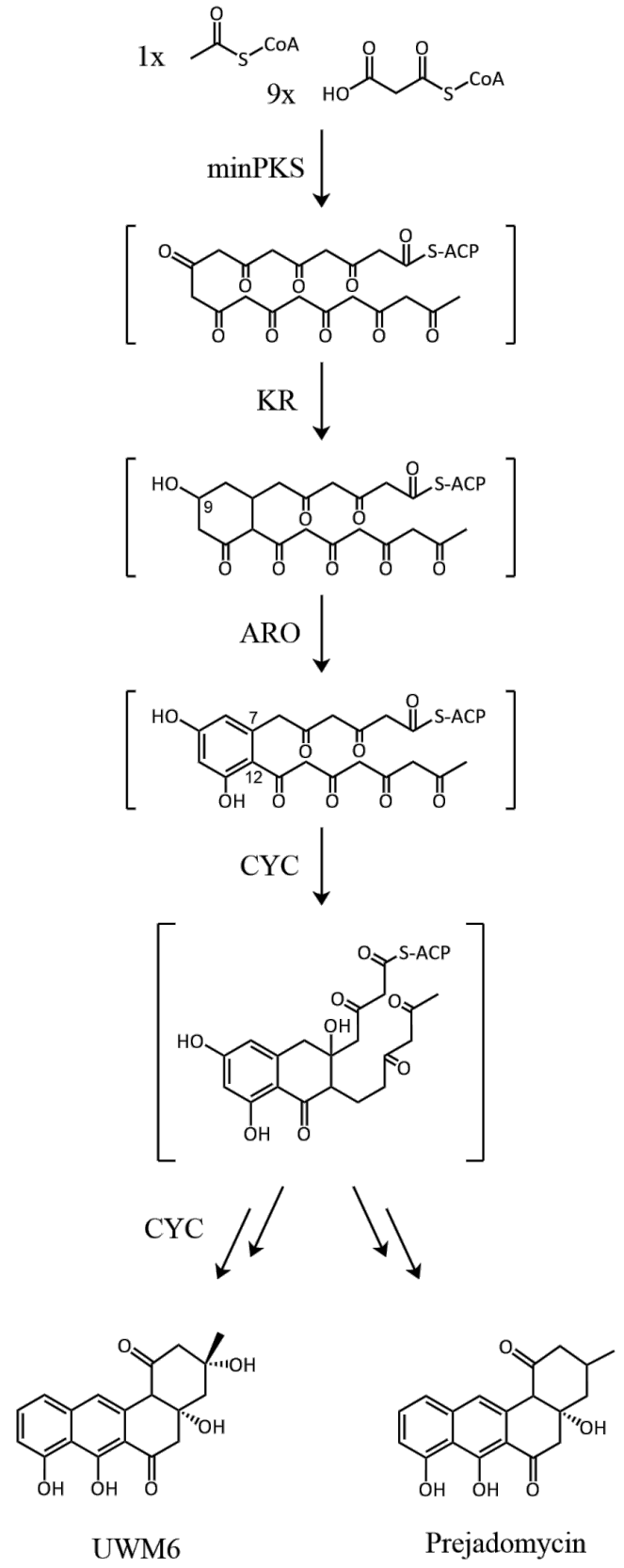

Figure 2. Angucycline biosynthesis. The iterative reaction between an acetyl-CoA starter unit and nine malonyl-CoA units via minPKS results in the formation of unstable intermediates, that are quickly converted into intermediates such as UWM6 and prejadomycin via ketoreductases (KR), aromatases (ARO), and cyclases (CYC).

Angucyclines are typically modified by flavoprotein monooxygenases (FPMO), antibiotic biosynthesis monooxygenases (ABM), and short-chain alcohol dehydrogenase/reductases (SDR) (Nuutila et al. 2024). The enzymes involved in these pathways are closely related and distributed in clusters in conserved order, as is shown in figure 3. For example, in the gaudimycin pathway, prejadomycin is hydroxylated at C12 and C12b by an NADPH dependent flavoprotein monooxygenase PgaE, present in the *pga* gene cluster in *Streptomyces* sp. PGA64. Then, an SDR enzyme CabV, originating from the *cab* cluster in *Streptomyces* sp. H021, produces gaudimycin C via a C6 ketoreduction (Kallio et al. 2011; Palmu et al. 2007). JadH is present in the jadomycin pathway and shares a significant amino acid sequence identity with PgaE (Patrikainen et al. 2012). Both use prejadomycin as a substrate for C12 hydroxylation. JadH does, however, carry an additional function in dehydration (Y. Chen et al. 2010). LanV from the landomycin pathway acts similarly to UrdMred and CabV (Mayer et al. 2005). Although the homology, these enzymes also share functional differences. Many enzymes in these pathways catalyze several reactions depending on various environmental factors highlighting their catalytic flexibility. Therefore, detailed *in vivo* and *in vitro* studies are essential in understanding specific enzymatic roles that depend on the biological context.

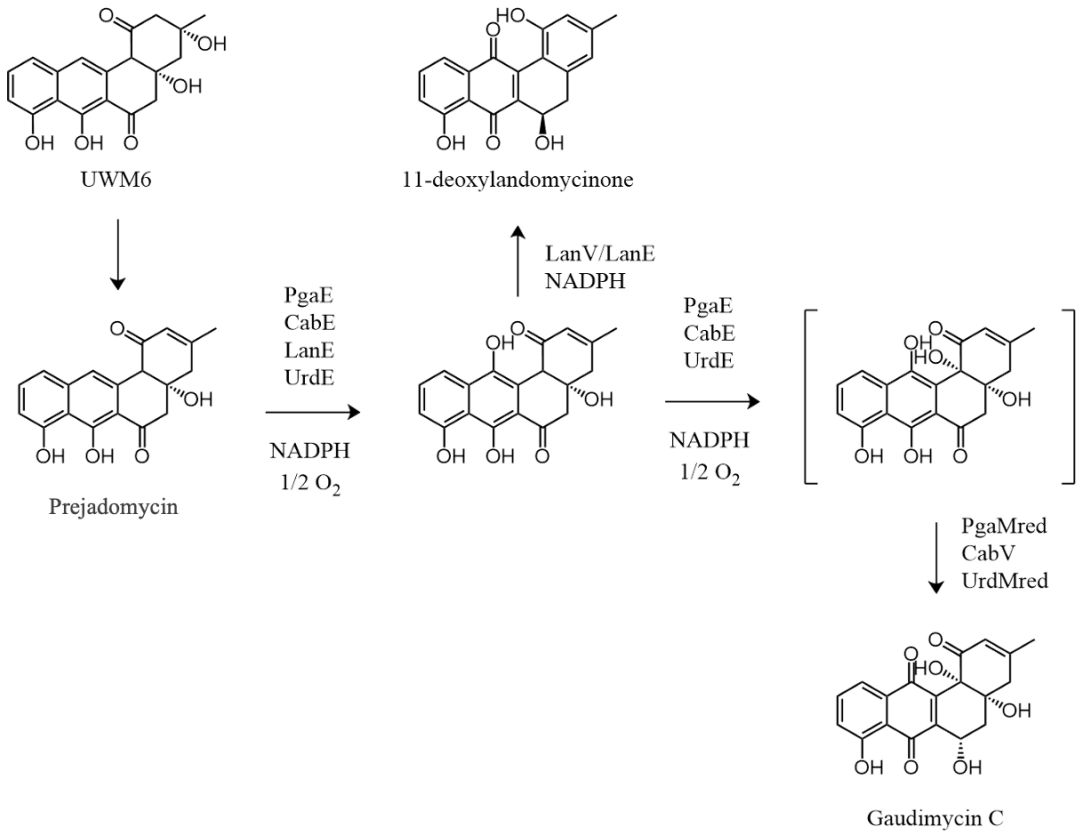

Figure 3. Typical angucycline redox reactions. The enzymes from *pga*, *cab*, *lan*, and *urd* gene clusters are highly related, and share common functions, including C12 hydroxylation by PgaE, CabE, LanE, and UrdE, and C6 ketoreduction by PgaMred, CabV, and UrdMred. Their activity results in common angucycline metabolites. Figure modified from Patrikainen et al. 2012.

1.3.1 Classical angucyclines

Classical angucyclines are characterized by their bent four-ring benz[*a*]anthracene scaffold synthesized by type II PKS. Classical angucyclines contain three linear B-, C-, and D-rings with the fourth A-ring attached in an angle, whereas non-classical angucyclines carry modifications or rearrangements in the core structure, such as addition, removal or cleavage of one of the rings. (Nuutila et al. 2024) The structure of the classical four-ring angucycline is shown in figure 4. In classical angucyclines, the structural diversity arises from the attachment of various groups such as sugar moieties in glycosylation, as well as hydroxylation, methylation, and acetylation. (Xu et al. 2025) Angucyclines without an attached carbohydrate group are referred to as aglycones or angucyclinones. The most well-known classical angucyclines include compounds like landomycins, as well as some gaudimycins and urdamycins. The most important and well-known example compound of each class are discussed here, although the diversity and amount of both classical and non-classical angucyclines is enormous (Kharel, Pahari, Shaaban, et al. 2012; H.-S. Liu et al. 2025; Xu et al. 2025).

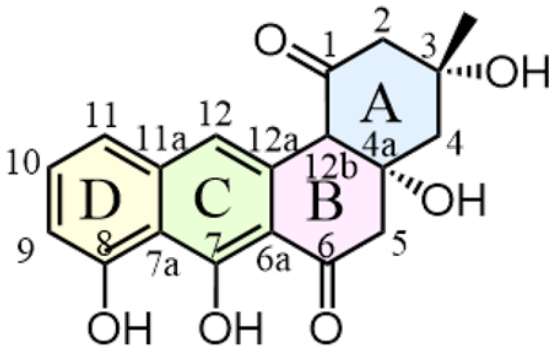

UWM6

Figure 4. The carbon atoms and rings of classical angucyclines. Classical angucyclines, such as UWM6, contain a tetracyclic structure with three linear rings, and the A-ring attached in an angle. Non-classical angucyclines feature a cleavage in one of the rings.

1.3.1.1. Landomycins

Landomycins are the largest and one of the most studied families within angucyclines (Kharel and Rohr 2012). Landomycin A, isolated from *Streptomyces cyanogenus* S136, and landomycin E, isolated from *Streptomyces globisporus*, are the most extensively studied, although others, such as landomycins B, C, and D, are also well characterized (Henkel et al. 1990). Landomycins are classic angucyclines characterized by a deoxysugar moiety of varying lengths attached to the aglycone, typically the C8 position, via *O*-glycosylation, as illustrated in figure 5 (X. Yang et al. 2011). They are produced through various redox tailoring reactions from prejadomycin, that is hydrolyzed and reduced to yield 11-deoxylandomycinone, which can then undergo further modifications (Yushchuk et al. 2019). The benz[*a*]anthraquinone backbone, to which the deoxy sugar is linked, can be, for example, landomycinone, 11-deoxylandomycinone, or tetrangulol, which are classical angucyclines with varying hydroxylation patterns. (Kharel, Pahari, Shaaban, et al. 2012) Landomycin A features an 11-hydroxylated landomycinone core with a hexasaccharide moiety containing four D-olivose and two L-rhodinose residues, making it the biggest known landomycin by molecular weight (Yushchuk et al. 2019). Landomycin E consists of a similar scaffold linked with a trisaccharide of two D-olivoses, and an L-rhodinose. In addition to their antibiotic activity, landomycins have showed anticancer properties. Landomycin A, for example, can disrupt the cell cycle and has shown activity against prostate cancer cell lines, whereas landomycin E appears as an

inducer of apoptosis and has shown promising activity in multiple drug-resistant cell lines (Kharel, Pahari, Shepherd, et al. 2012; Luzhetskyy et al. 2005).

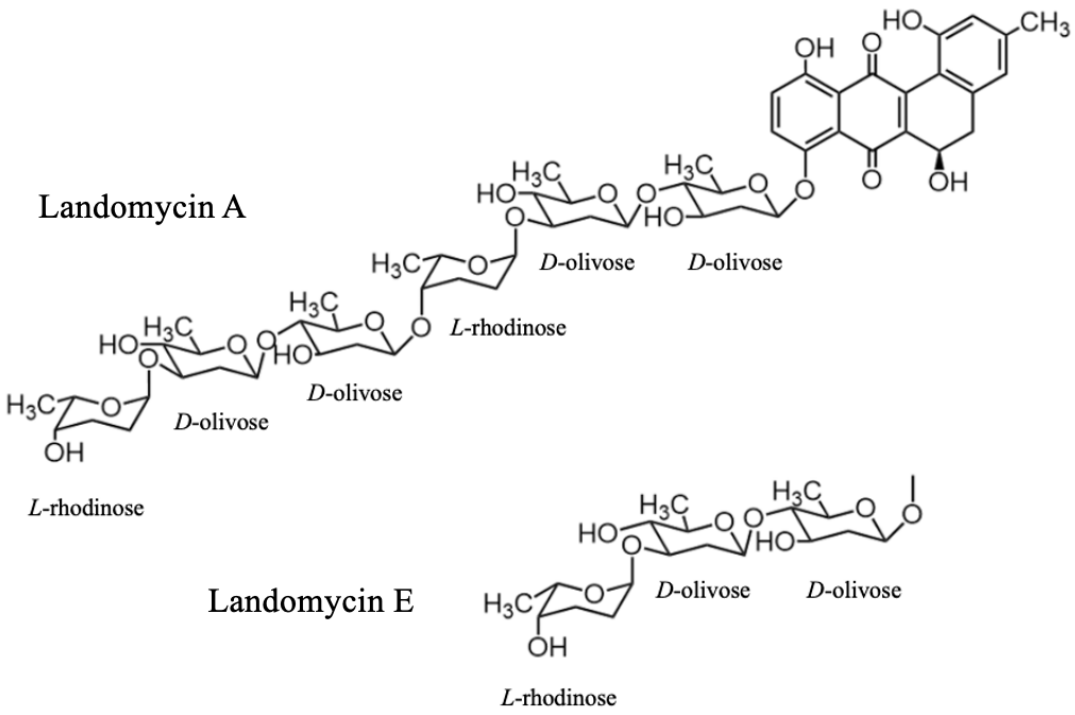

Figure 5. Common landomycin structures. Landomycin A is presented above and features a landomycinone benz[*a*]anthraquinone scaffold with an *O*-linked hexasaccharide moiety at C8 position. Landomycin E has a similar aglycone but is linked with a trisaccharide.

The tailoring enzymes involved in the landomycin biosynthesis pathway are thoroughly studied and well-known in both *in vivo* and *in vitro* (Kharel, Pahari, Shaaban, et al. 2012). The *lan* gene cluster, initially cloned from *S. cyanogenus* S136, consists of type II polyketide genes, post-polyketide tailoring enzymes, sugar biosynthetic genes, glycosyltransferases, as well as regulatory and antibiotic transport genes, although other landomycin-producing gene clusters have also been identified (Kharel, Pahari, Shepherd, et al. 2012). The gene clusters in the landomycin A producing *S. cyanogenus* S136 (*lan*), and landomycin E producing *S. globisporus* (*lnd*) are almost identical (Zhu et al. 2005). After the biosynthesis of the angucycline scaffold by type II PKS, the framework undergoes various oxidation, reduction, and sugar transfer reactions (Yushchuk et al. 2019). The post-PKS tailoring process involves oxygenases LanE and LanZ5, reductases LanV, LanZ4, and LanO, an oxidoreductase LanM2, along with four glycosyltransferases LanGT1-4. LanM2 is an oxidoreductase responsible for the 2,3-dehydration step yielding prejadomycin, and likely catalyses the first step of the pathway. (Kharel, Pahari, Shaaban,

et al. 2012) The closely related LndM2 from the *lnd* pathway is bifunctional and has additional functions to the 2,3-dehydration on two reaction pathways, both yielding 11-deoxylandomycinone. In the first pathway, LndM2 is responsible for C6 hydroxylation, followed by reduction of a C5-C6 double bond and 2,3-dehydration. Alternatively, LndM2 can reduce the C5-C6 double bond, after which it oxygenates C6 resulting in aromatization (H.-S. Liu et al. 2025). In the biosynthesis of landomycinone and 11-deoxylandomycinone, LanE and LndE catalyze oxidation at C12, as is shown in figure 6. After both LanM2 and LanE, or the corresponding *lnd* pathway enzymes, LanV catalyses the reduction of a C6 ketogroup. Lastly, LanZ4 and LanZ5 together catalyze the hydroxylation step at C11. LanZ4 is a reductase that provides the reduced flavin (FMNH) cofactor, while LanZ5 is a bifunctional oxygenase-dehydratase that carries out an oxygenation reaction using the reduced cofactor. LanZ4 and LanZ5 have a broad substrate specificity, and the hydroxylation can occur at different glycosylation stages. (Kharel, Pahari, Shaaban, et al. 2012; Kharel, Pahari, Shepherd, et al. 2012).

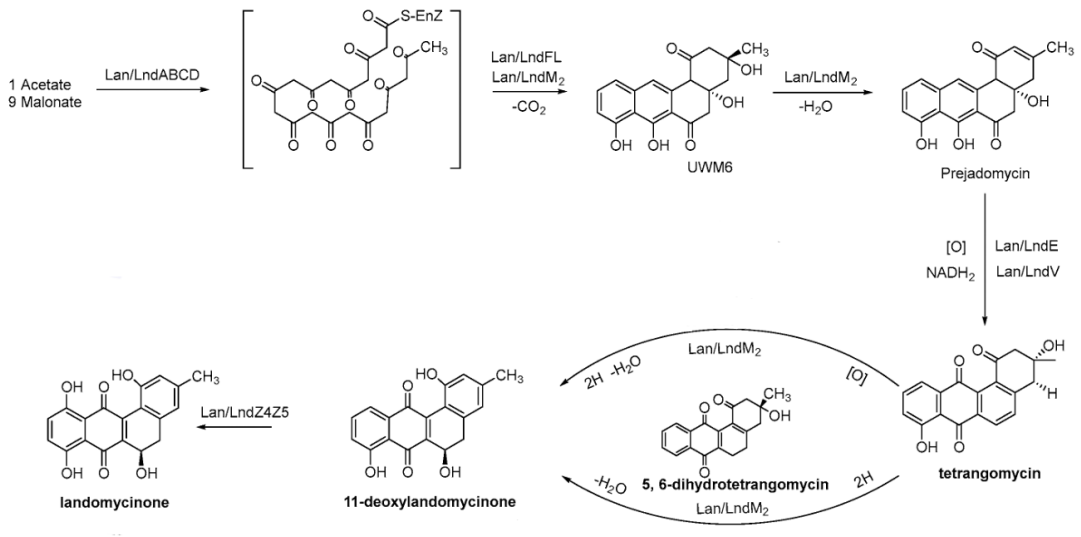

Figure 6. Landomycinone and 11-deoxylandomycinone biosynthesis. The landomycin aglycones are formed when by a type II PKS product UWM6 is dehydrated by LanM2/LndM2 to yield prejadomycin, which LanE/LanV then convert to tetrangomycin. From there, two parallel tailoring pathways may occur, leading to 11-deoxylandomycinone and landomycinone, both of which can be glycosylated to form the final landomycin structures.

Several NDP-hexose-dehydratases, such as *lanG*, *lanS*, and *lanR*, and an oxidoreductase *lanT* are associated with the biosynthesis of the deoxysugars. Low substrate specificity containing glucosyltransferases (GT), such as LanGT2, are responsible for the addition of sugar moieties into the landomycin scaffold, after which the LanZ4/LanZ5 catalyzed

C11 hydroxylation likely occurs (Yushchuk et al. 2019). The sugar moiety is further modified by LanGT1 and LanGT4, that facilitate the formation of the trisaccharide chain of landomycin E. Remarkably, LanGT1 and LanGT4 are used twice in the pathway, as the hexasaccharide unit is synthesized by further extension of the trisaccharide via LanGT3, LanGT1, and LanGT4 in the biosynthesis of landomycin A. Due to their relaxed substrate specificity, these enzymes are highly researched, and represent a great potential in applications with glycodiversification of natural products. (Kharel, Pahari, Shepherd, et al. 2012; Yushchuk et al. 2019)

1.3.1.2. Urdamycins A and B and gaudimycins A-C

Urdamycins and gaudimycins can be categorized as either classical or non-classical depending on the type. Urdamycins A and B, for example, are classical angucyclines with a *C*- or *O*-glycosidically linked saccharide side chains, that were discovered from *Streptomyces fradiae* Tü2717 in mid to late 1980's (Rohr et al. 1989). Alongside landomycins, they have been under extensive research since their discovery due to their promising clinical properties. Similarly to many other angucycline classes, they act as antimicrobials and carry anticancer properties (Drautz et al. 1986). Urdamycins A and B feature the characteristic polyaromatic benz[*a*]anthacene aglycone core typical of angucycline antibiotics and are glycosylated with deoxysugar moieties, as shown in figure 7. Both contain a trisaccharide with two *O*-glycosidically linked L-rhodinoses and a *C*-glycosidically linked D-olivose. In addition, urdamycin A carries an *O*-linked D-olivose. The sugar moieties are linked to the aglycone via four glycosyltransferases, urdGT1a, urdGT1b, and urdGT1c introducing sugars through *O*-glycosylation, as well as urdGT2 that mediates *C*-glycosidic bond formation. (Kharel, Pahari, Shepherd, et al. 2012)

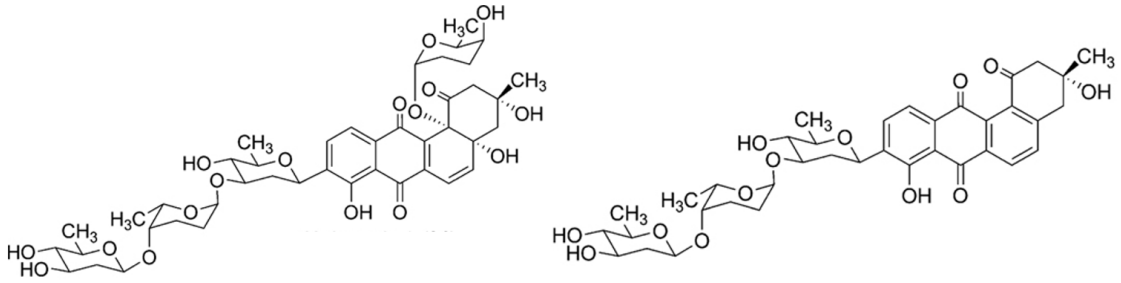

Figure 7. Structures of urdamycins A and B. Urdamycins A and B represent classical angucyclines with an intact tetracyclic core, to which the deoxysugar moieties are attached. Urdamycin A contains a trisaccharide similarly to urdamycin B but also carries an additional D-olivose. Figure modified from Kharel, Pahari, Shepherd, et al. 2012.

Similarly to landomycins, the urdamycin gene cluster (*urd*) contains genes responsible for the polyketide synthesis, post-PKS modifying, sugar biosynthesis, as well as glycosyltransferase, regulatory, and transporter genes. Additionally, the sequences share a high level of sequence identity with the corresponding genes from the landomycin gene cluster. (Faust et al. 2000)

Gaudimycins were identified in 2007 through heterologous expression. Gaudimycin A was produced via a cryptic *pga* gene cluster isolated from *Streptomyces* sp. PGA64 and Gaudimycin B was similarly discovered when expressing the highly related cryptic *cab* gene cluster from *Streptomyces* sp. H021. Both gaudimycins A and B consist of a benz[*a*]anthracene skeleton similarly to urdamycins, with the main difference between gaudimycins A and B being the lack of a hydroxy group at C6 position in gaudimycin A. (Palmu et al. 2007) Gaudimycin C was discovered by the activity of the *pga* cluster genes *in vitro*, and its structure strongly resembles that of gaudimycin B as the structures are diastereomers. (Kallio et al. 2008) The structures of gaudimycins A, B, and C are presented in figure 8.

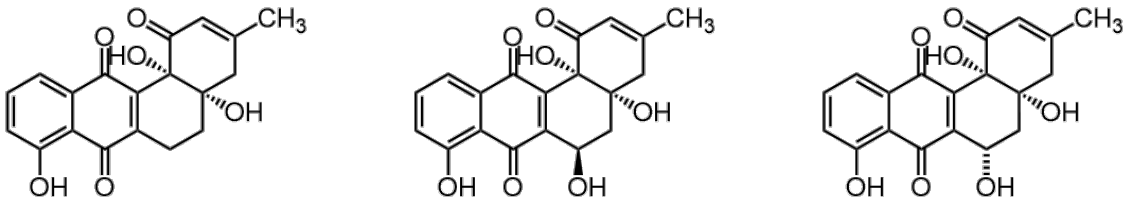

Figure 8. The structures of gaudimycins A-B. Type A-C gaudimycins represent classical angucyclines with an intact tetracyclic benz[*a*]anthracene core. Gaudimycin A lacks a C6 hydroxy group, whereas gaudimycin B and C are diastereomers.

The genes encoding for both urdamycin and gaudimycin pathway intermediates are closely related to those of landomycin and therefore share functional similarly (Patrikainen et al. 2012). One of the first common post-PKS tailoring step in angucycline biosynthesis is the hydroxylation of prejadomycin via a flavin-dependent monooxygenase, such as LanE, CabE, UrdE and PgaE, in a reaction that requires NADPH and oxygen. The subsequent reaction depends on the pathway. Tailoring enzymes LanM2, PgaM and UrdM act as fusion proteins with several functions, containing a C-terminal SDR domain and an N-terminal flavin-dependent oxygenase domain. The flavin-dependent oxygenase CabV and SDR CabM together carry similar activities, as they are homologous to the oxygenase and reductase domains of the fusion proteins. (Kallio et al. 2011) In addition, the SDR domains of the fusion proteins contain an internal start codon and proteins can therefore act independently as reductases, similarly to CabM (Kallio et al. 2008). LanV from the landomycin pathway is homologous to CabV and is also expressed independently. After the subsequent C12 and C12b hydroxylation steps on prejadomycin by PgaE, gaudimycin C is produced via a stereospecific C6 ketoreduction by CabV, or the reductase domain of the two-domain PgaM, also known as PgaMred, in a strictly coupled reaction. However, if PgaE is replaced by LanV, prejadomycin is not transformed into gaudimycin C if but rather 11-deoxylandomycinone, showing strict substrate specificity regarding the C12b hydroxylation. (Fan and Zhang 2018). Urdamycin biosynthesis occurs in similar order with homologous genes, as UrdE performs consecutive hydroxylations at positions C12 and C12b similarly to PgaE, after which C6 ketoreduction occurs via the reductase domain of the two-domain UrdM, again similarly to CabV and PgaMred. (Patrikainen et al. 2012) After the initial angucycline aglycone is constructed, sugar moieties may be added to the core structure via glycosyltransferases, similarly to landomycins (Kharel, Pahari, Shepherd, et al. 2012).

1.3.2 Non-classical angucyclines

Non-classical or atypical angucyclines are characterized by modifications on the core structure itself, leading to ring opening, rearrangement, or partial cleavage of one or more rings (Nuutila et al. 2024). They arise from the same type II PKS pathway as classical angucyclines yielding the typical benz[*a*]anthracene core structure but later acquire unusual scaffolds with, for example, linear tetracyclic or tricyclic systems via enzymatic and non-enzymatic modifications (H.-S. Liu et al. 2025). Non-classical angucyclines carry even more structural diversity compared to classical structures, and can therefore exhibit unique functions (Tibrewal et al. 2012). Cleavage can occur in any of the rings of the tetracyclic scaffold, although D-ring-cleaved structures are rare, and the mechanistic details of their biosynthesis remain poorly characterized, whereas rearrangements in rings A and B are relatively common. The cleavage of angucycline rings requires a chemically challenging breakage of a C-C bond. While the cleavage reaction is crucial to the biological function of the molecule, the mechanism and order in which it occurs is generally not fully determined. The reaction is, however, often catalyzed by two families of enzymes, FAD-dependent and ring opening monooxygenases. The FAD-dependent monooxygenases, including LanE, CabE, UrdE and PgaE, act early on in the pathway catalyzing reactions such C12 and C12b hydroxylation and 4a/12b dehydration, whereas the ring-opening oxygenases catalyze the oxidative C-C bond cleavage followed by various rearrangement reactions. (Fan and Zhang 2018) Gaudimycin D, jadomycin, and lugdunomycin, for example, carry a cleavage in the A-, B-, and C-rings, respectively, followed by drastic rearrangements to result in structures that yield their biological properties (Fan et al. 2012; Guo et al. 2015; Wu et al. 2019). The structures are shown in figure 9. The study of rearranged angucyclines is important, as it can be extremely useful in understanding the total biosynthesis of angucyclines (Mikhaylov et al. 2021).

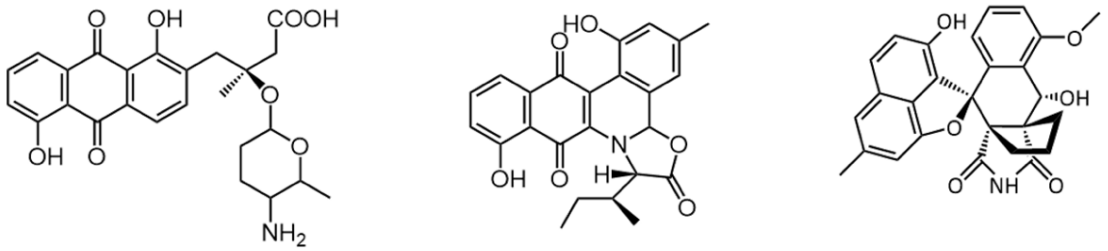

Figure 9. Structures of non-classical angucyclines. Gaudimycin D, jadomycin, and lugdunomycin feature a cleavage in the A-, B-, and C-rings, respectively.

The non-classical angucyclines represent a major branching point in angucycline post-PKS biosynthesis, as the early steps and the intermediates such as UWM6 and prejadomycin, are shared between classical and non-classical pathways. In non-classical angucycline biosynthesis, prejadomycin is often modified via C12-hydroxylation and 4a-12-dehydration reactions into dehydrorabelomycin, which is a key intermediate in many pathways (Fan and Zhang 2018). When synthesizing non-classical angucyclines, the pathways diverge to yield a wide variety of end-products, often with unique and complex structures. The specific reaction mechanisms and intermediate compounds involved in ring cleavage vary depending on which ring is targeted. (Kharel, Pahari, Shepherd, et al. 2012)

In the case of A-ring cleavage, as observed in the biosynthesis of, for example, gaudimycins D and E, the pathway is proposed to proceed via Baeyer-Villiger oxidation yielding a lactone intermediate that undergoes hydrolytic cleavage to open the ring (Guo et al. 2015; Rix et al. 2005). Baeyer-Villiger monooxygenases (BVMO) catalyze Baeyer-Villiger oxidations of ketones and cyclic ketones into esters or lactones, respectively, by inserting an oxygen atom into a C-C bond adjacent to a carbonyl group with NAD(P)H (Tolmie et al. 2019). Baeyer-Villiger oxidations are present in many pathways yielding non-classical angucyclines with an opened ring. The FAD-dependent monooxygenases catalyze B-ring cleavage through C5 hydroxylation, which is followed by Baeyer-Villiger oxidative cleavage at the adjacent C6 ketogroup, leading to opening of the B-ring (Tibrewal et al. 2012).

The mechanisms underlying opening rings C and especially D are less well-known, which is why structures with rearrangements in D-ring are not discussed here. The biosynthesis

of the C-ring cleaved compound lugdunomycin requires an 8-*O*-methylated substrate, which is likely further modified via 6a/12a epoxidation (Elsayed et al. 2023; Nuutila et al. 2024). Dimeric angucyclines, in which two monomeric angucycline-derived units are joined, also exist, further expanding the chemical variety in the family of non-classical angucyclines. Lomaiviticins and difluostatins are examples of such compounds. (Huang et al. 2018)

1.3.2.1. Angucyclines with rearrangements in the A-ring

Although some gaudimycins and urdamycins are classified as classical angucyclines, both groups also include non-classical compounds, such as the A-ring cleaved urdamycins C–E and gaudimycins D and E (Guo et al. 2015; Rohr 1989). The A-ring cleavage is suggested to proceed via a Baeyer–Villiger oxidation, in which a flavin-dependent monooxygenase incorporates an oxygen atom into the aglycone ring, forming a transient lactone intermediate. This intermediate can then undergo rearrangements and hydrolysis, ultimately leading to cleavage of the A-ring and formation of tricyclic structures with an open-ring system (Guo et al. 2015).

The Baeyer–Villiger oxidation mechanism has also been suggested to be involved the formation of urdamycin L, a non-classical angucycline, originally identified in *Streptomyces fradiae* TÜ 2717, that contains a modified A-ring with a six-membered cyclic ester, also known as an ε lactone (Rix et al. 2003). Urdamycin L is a shunt product that provides direct evidence of the surprising action of urdamycin pathway enzyme, UrdM, and therefore allows insights into the mechanisms of Baeyer-Villiger oxidation. Based on its sequence, UrdM is a bifunctional enzyme with an N-terminal flavin-dependent oxygenase domain, and a C-terminal reductase domain, similarly to PgaM and LanM2 (Faust et al. 2000; Kharel, Pahari, Shepherd, et al. 2012). Urdamycin L biosynthesis is presented in figure 10.

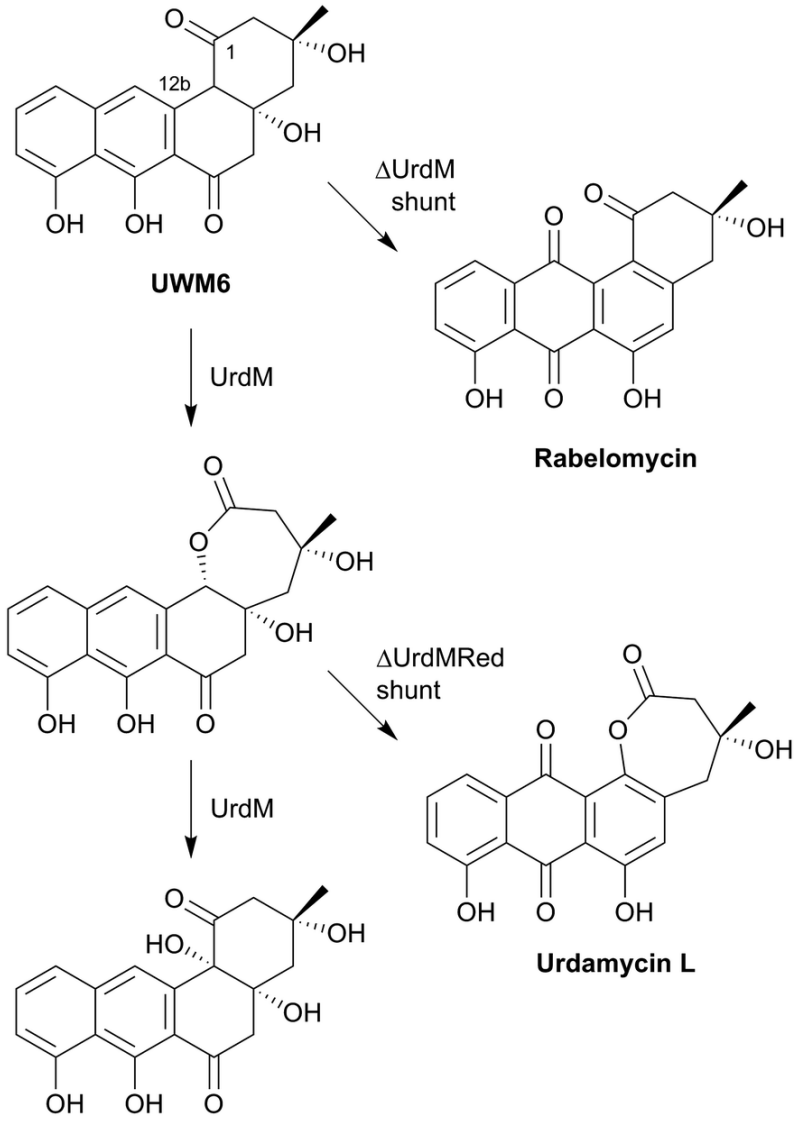

Figure 10. Formation of shunt product urdamycin L. Deletion of the UrdM reductase domain allows Baeyer–Villiger oxidation by the remaining oxygenase, yielding urdamycin L with a lactonized A-ring, and likely a spontaneous C12b hydroxylation. Full *urdM* deletion results in rabelomycin with an intact tetracyclic core. Figure from Tolmie et al. 2019.

The discovery of urdamycin L resulted in clarifying the biological roles of the two domains of UrdM in the biosynthesis of urdamycins. Urdamycin L, featuring a C12b hydroxyl group, was found in an *urdM* deletion mutant, which was initially unexpected, as UrdM was previously thought to catalyze this C12b oxygenation step. However, a more targeted in-frame deletion mutant affecting only the C-terminal reductase domain resulted in the loss of hydroxylase activity, again leading to the formation of urdamycin L in small amounts (Tolmie et al. 2019). This suggests that the N-terminal oxygenase domain of UrdM retains some Baeyer-Villiger oxidation activity on precursor UWM6 but is unable to carry out subsequent tailoring steps. (Kharel, Pahari, Shepherd, et al. 2012; Rix et al. 2003)

The Baeyer-Villiger oxidation tailoring step is thought to shift the biosynthetic pathway towards urdamycin L rather than classical tetracyclic products such as urdamycin A. The hydroxyl group at C12b is thus likely introduced spontaneously after the oxidation, rather than through direct enzymatic hydroxylation, as was previously assumed (Kharel, Pahari, Shepherd, et al. 2012). Additionally, a full Δ*urdM* knockout mutant accumulates the common angucycline shunt product rabelomycin, which retains an intact tetracyclic structure, further supporting the role of UrdM in catalyzing A-ring opening via Baeyer-Villiger oxidation. The C-terminal reductase domain of UrdM is suggested to be responsible for the base-assisted rearrangement that restores the intact A-ring during the biosynthesis of urdamycin A (Kharel, Pahari, Shepherd, et al. 2012; Tolmie et al. 2019).

Gaudimycin D and E were discovered from *Streptomyces* sp. PGA64 through targeted activation of the whole cryptic *pga* gene cluster, which had previously been only partially expressed (Guo et al. 2015). The biosynthesis of gaudimycin D resembles that of urdamycin L, as gaudimycin D is similarly formed via a Baeyer-Villiger oxidation leading to the formation of an ε lactone containing intermediate, as illustrated in figure 11. The substrate for synthesizing gaudimycin D is, however, prejadomycin rather than UWM6. (Pahari, Kharel, Shepherd, van Lanen, et al. 2012) The ε lactone intermediate undergoes hydrolysis to yield a tricyclic intermediate structure with an opened A-ring. Subsequent tailoring steps, including two hydrations, the reintroduction of a hydroxyl group, and the attachment of deoxysugar units, complete the structure of gaudimycins D and E (Guo et al. 2015). Still, it is suggested, that the glycosylation reactions might occur prior to lactone formation in similar pathways, but the order might vary depending on enzyme specificity (Kharel, Pahari, Shepherd, et al. 2012). With the open-ring structure, the aglycone moiety of non-classical gaudimycins D and E differ from those of classical gaudimycins A-C. Notably, the ε lactone intermediate can also be rearranged without hydrolysis to form gaudimycin C with an intact tetracyclic structure by PgaMred. (Guo et al. 2015)

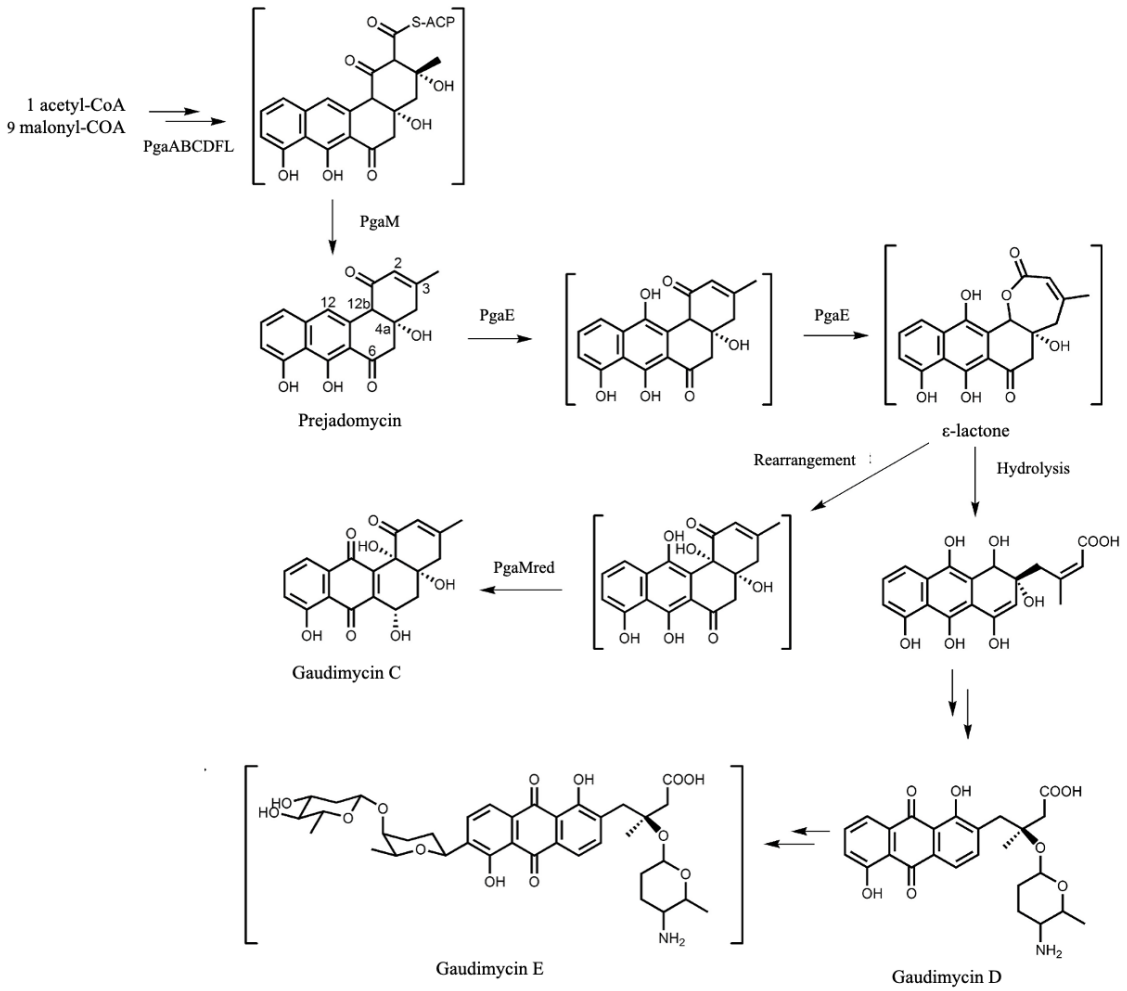

Figure 11. Synthesis of gaudimycins E and D. Prejadomycin undergoes a Baeyer-Villiger oxidation to form an ε lactone-containing intermediate. This intermediate can either be rearranged by PgaMred to yield the classical angucycline gaudimycin C or hydrolyzed to produce the non-classical angucyclines gaudimycins D and E with an opened A-ring. Figure modified from Guo et al. 2015.

Urdamycins C-E and H are similarly characterized by modifications in the aglycone itself and therefore classified as non-classical. Urdamycins C, D, and E carry additional structural elements likely derived from amino acids tyrosine, tryptophan, and methionine, respectively, and are synthesized from urdamycin A. Urdamycin H, also featuring a tyrosine-derived chromophore, was discovered after urdamycins C-E (Rohr 1989). The amino-acid derived moieties are likely introduced to the aglycone after the attachment of sugars, and might happen non-enzymatically (Pahari, Kharel, Shepherd, van Lanen, et al. 2012). The chromophores urdamycins C-E and H carry give them unique colouring, therefore distinguishing them from other common angucycline antibiotics. The classical angucycline urdamycin A contains a hydroxynaphthoquinone chromophore and therefore exhibits a typical orange colour, while urdamycins C and D, for example, show dark red and blue discoloration, respectively (Rohr 1989). Despite differences in the aglycones, the sugar moieties remain same between urdamycins C-H and E, and urdamycin A

(Drautz et al. 1986). By contrast, urdamycin F, also classified as a non-classical angucycline, exhibits A-ring hydration and structural rearrangement typical to non-classical angucyclines, such as urdamycin L, but both lack an amino-acid derived chromophore (Rohr and Zeeck 1987). Urdamycin F also contains a sugar unit different to those of urdamycins A, C-E, and H. The structures are presented in figure 12.

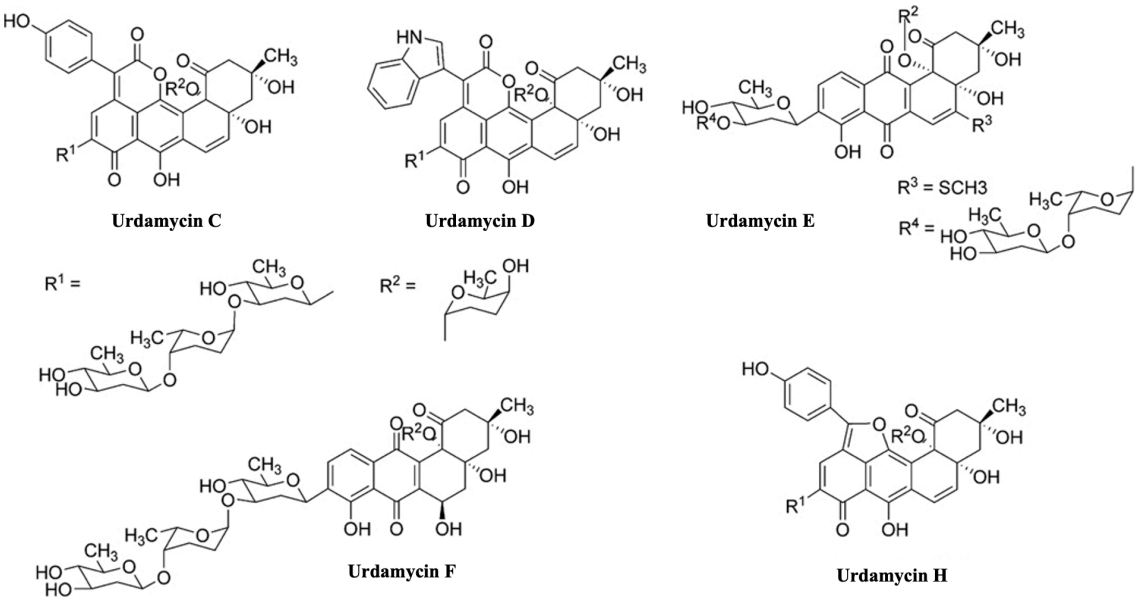

Figure 12. Structures of urdamycins C-F and H. Urdamycins C-E and H feature similar deoxysugar moieties and amino-acid derived chromophores giving them unique colouring. Alternatively, urdamycin F consists of a hydrated A-ring without a distinguishable chromophore, as well as a different sugar unit compared to those of urdamycins C-E and H. Figure modified from Kharel, Pahari, Shepherd, et al. 2012.

Other urdamycins derivatives with ring A modifications such as Baeyer-Villiger-type modifications, arising from pathway engineering and gene deletions, have also been identified (Kharel, Pahari, Shepherd, et al. 2012). Deleting glycosyltransferase *urdGT2*, for example, results in the formation of urdamycins I, J, and K that lack the *C*-connected sugar (Faust et al. 2000). These derivatives help understand the role of glycosylation in the biosynthesis of angucyclines.

1.3.2.2. Angucyclines with rearrangements in the B-ring

The B-ring is the centremost aromatic structure in angucyclines, and therefore alterations on it will change the overall structure of the compound significantly. Jadomycins, gilvocarcins, kinamycins, lomaiviticins, and fluostatins, for example, are synthesized via an oxidative B-ring opening and subsequent rearrangement (Fan and Zhang 2018). The mechanisms in which these modifications occur do often vary from those of ring A.

However, both may feature oxidative ring-cleavage via Baeyer-Villiger oxidation. The C-C bond cleavage involved in B-ring opening during the biosynthesis of non-classical angucyclines jadomycin, kinamycin, and gilvocarcin are all proposed to occur via Baeyer-Villiger oxidation catalyzed by unique ring-opening oxygenases. The ring-opening is followed by structural rearrangements that yield the final structure of these unique compounds. (Kharel, Pahari, Shepherd, et al. 2012)

Jadomycins are among the earliest and most studied angucycline antibiotics (Kharel, Pahari, Shepherd, et al. 2012). They are synthesized from prejadomycin in *S. venezuelae* ISP5230 in tailoring reactions involving several oxygenases such as an JadF, an antibiotic biosynthesis monooxygenase JadH, and a unique ring-opening oxygenase JadG. Although dependent on flavin cofactors, more recent studies classify JadG to the antibiotic biosynthesis monooxygenase superfamily of proteins similarly to JadH (Nuutila et al. 2024). The biosynthesis yields jadomycin B, and its aglycone jadomycin A, both containing a nitrogen-containing pentacyclic benz[*b*]oxazolophenanthridine ring system (Y.-H. Chen et al. 2005; Fan and Zhang 2018). The biosynthesis of jadomycins proceeds via two initial dehydration steps at C2-3 and C4a-12b, followed by an oxygenation at C12. Next, the ring-opening oxygenase JadG catalyses C5 hydroxylation of the angucycline core in a $FADH_2$-dependent reaction and promotes oxidative cleavage with the incorporation of an L-amino acid, such as L-isoleucine in the case of jadomycin A, via a nucleophilic attack (Tibrewal et al. 2012). The ring-opening occurs via a Baeyer-Villiger type mechanism, eventually resulting in the formation of an ε lactone intermediate. (Y.-H. Chen et al. 2005; Kharel, Pahari, Shepherd, et al. 2012; Rix et al. 2005) The aglycone modifying reactions are followed by glycosylation (Kharel, Pahari, Shepherd, et al. 2012; K. Yang et al. 1996). The biosynthetic pathway of jadomycins highly resembles that of kinamycins and gilvocarcins (Fan and Zhang 2018). However, closer inspection of JadF and JadH reveals surprising functions.

The oxygenases JadF and JadH possess an additional dehydratase activity (Kharel, Pahari, Shepherd, et al. 2012). Along with acting as oxygenases, JadF and JadH catalyze the initial 2,3-dehydration and 4a,12b-dehydrations, respectively, yielding dehydrorabelomycin. Therefore, although the sequence identity, JadH performs different functions than the homologous FAD-dependent monooxygenases such as PgaE, UrdE, and LanE and is rather classified as an antibiotic synthesis monooxygenase. (Y. Chen et al. 2010; Nuutila et al. 2024; Patrikainen et al. 2012). In addition, it is suggested that,

although being an oxygenase, JadF might not have a role in the oxidation process but rather, has a crucial role at the beginning steps of post-PKS tailoring by catalyzing the 2,3-dehydration step (Pahari, Kharel, Shepherd, van Lanen, et al. 2012). Based on sequence analysis, JadG is characterized as an anthrone oxygenase catalyzing C12 oxygenation. Interestingly, C12 oxygenation also occurs in deletion mutants lacking *jadG*, suggesting that instead of JadG, JadH might be responsible for the oxygenation step. The dehydration and C12 oxygenation form an intermediate called CR1. (Kharel, Pahari, Shepherd, et al. 2012) The proposed pathway is presented in figure 13. However, the exact order and mechanism of the oxygenation and ring opening remain unclear, and therefore the oxygenation process is often referred to as the "biosynthetic black box".

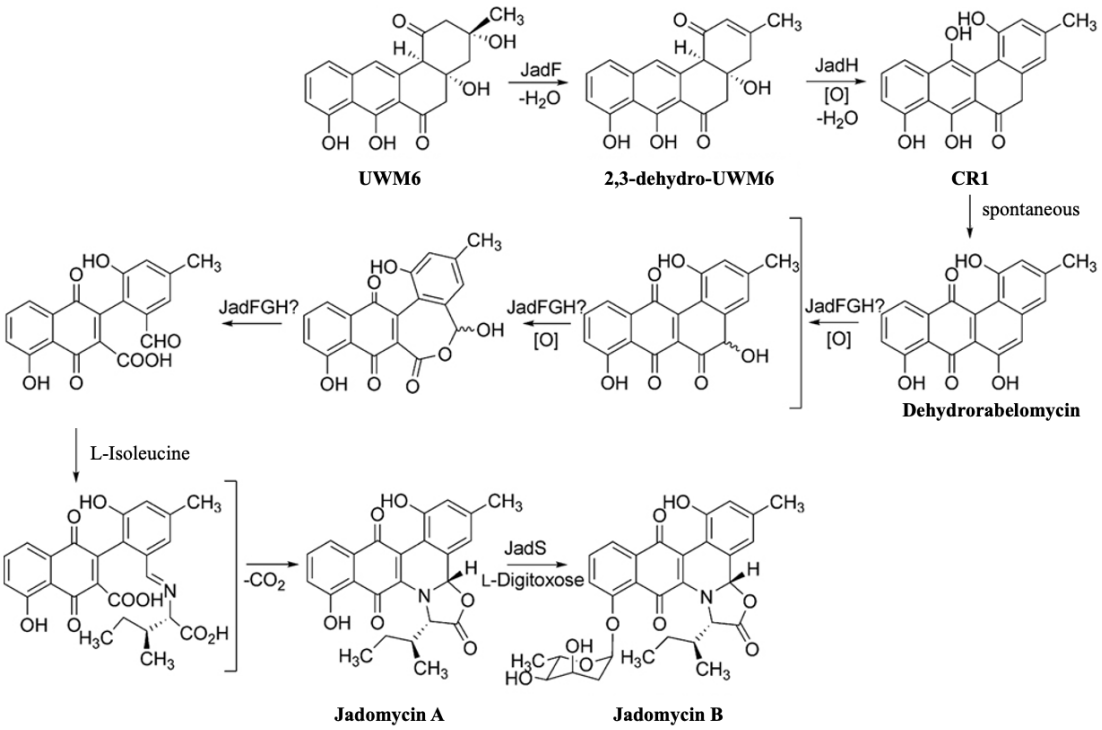

Figure 13. The proposed biosynthesis pathway of jadomycins A and B. The biosynthesis involves sequential 2,3- and 4a,12b-dehydration steps by JadF and JadH, respectively, as well as an C12 oxygenation of UWM6 to yield CR1. The subsequent oxidative cascade, including the incorporation of L-isoleucine, the cleavage of the B-ring, and the formation of jadomycin B and its aglycone jadomycin A, remains unclear. Figure modified from Kharel, Pahari, Shepherd, et al. 2012.

Several jadomycin analogues with varying amino acids also exist to further expand the versatility of this angucycline subgroup. For example, jadomycin V, M, T, and G, contain L-valine, L-methionine, L-threonine, and L-glycine, respectively. Similarly to urdamycins C-E and H, the incorporation of amino acids is suggested to occur non-enzymatically, as all natural amino acids are able to be fused into the aglycone regardless

of the structural similarity, creating novel analogues of jadomycin B (Rix et al. 2004). The biosynthesis and attachment of deoxysugar moieties, such as L-digitoxose in jadomycin B, are mediated by the JadS glycosyltransferase, supported by several reductases and nucleotide sugar synthases responsible for producing the activated sugar donors (Kharel, Pahari, Shepherd, et al. 2012).

Gilvocarcins V, M, and E, also referred to as gilvocarcin-type aryl-C-glycosides, are among the most important examples of a unique class of the well-known anticancer antibiotics, gilvocarcins. The biosynthetic pathway of many gilvocarcins resembles that of jadomycins (Fan and Zhang 2018). Gilvocarcins were first isolated from *S. anandii* (C-22437) but are found as a metabolite in various *Streptomyces* species (Balitz et al. 1981; Pahari, Kharel, Shepherd, van Lanen, et al. 2012). Several analogues have been found, and all contain the characteristic polyketide-derived benzo[*d*]naphtho[1,2-*b*]pyran-6-one chromophore formed via a complex oxidative rearrangement process but vary in the *C*-glycosidically attached sugar units. Gilvocarcin V, for example, features a vinyl group side chain at C8, and a *C*-glycosidically linked D-fucofuranose at C4 (T. Liu et al. 2006). Various gilvocarcin analogues exist beyond V, M, and E, including less-characterized variants like gilvocarcins B, C, T, as well as defucogilvocarcins, that lack a sugar unit. The main differences between the various analogues lie mainly in side-chain modifications and glycosylation patterns. (Pahari, Kharel, Shepherd, van Lanen, et al. 2012) Common examples of gilvocarcin structures are presented in figure 14.

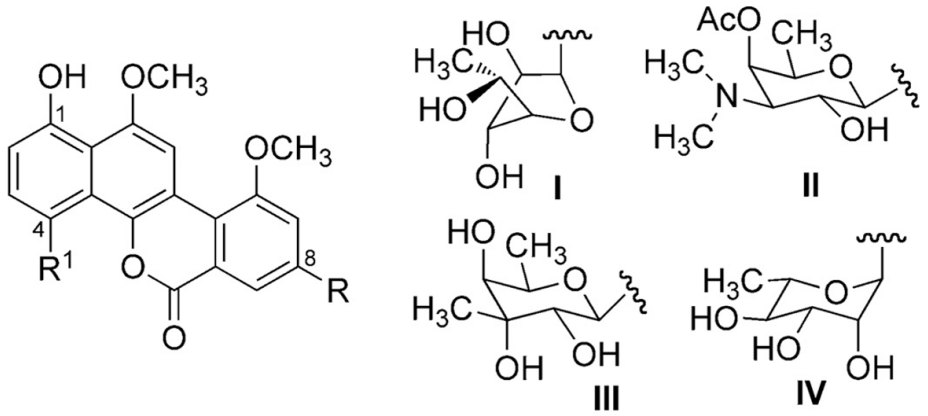

R = CH_3, R^1 = H: defucogilvocarcin M
R = $CH{=}CH_2$, R^1 = H: defucogilvocarcin V
R= CH_3, R^1 = I: gilvocarcin M
R= $CH{=}CH_2$, R^1 = I: gilvocarcin V
R= CH_2CH_3, R^1 = I: gilvocarcin E
R= $CH{=}CH_2$, R^1 = II: ravidomycin V
R= $CH{=}CH_2$, R^1 = III: chrysomycin V
R= $CH{=}CH_2$, R^1 = IV: polycarcin V

Figure 14. Common gilvocarcin structures. Gilvocarcins share a core aglycone structure but differ in their attached groups. They typically feature a sugar unit at C4 position, such as D-fucofuranose in gilvocarcin V, a D-ring ε lactone formed via Baeyer-Villiger oxidation, and various side chains at C8 position. Figure modified from Pahari, Kharel, Shepherd, van Lanen, et al. 2012.

Gilvocarcins are known to have a strong anti-tumour capacity, a unique mode of action, and, unlike many other angucyclines, a remarkably low toxicity. However, they are poorly soluble, which remains an obstacle in their development as therapeutics. (Pahari, Kharel, Shepherd, van Lanen, et al. 2012) Gilvocarcin V is known to mediate the cross-linking between DNA and the histone complex domain H3 in a unique manner, thus presenting as an interesting anticancer agent (T. Liu et al. 2006) However, similarly to many other ring-cleaved angucyclines, the exact mechanism of the biosynthesis of gilvocarcins is only partially understood. Many gilvocarcins involve the Baeyer-Villiger oxidation at the C12 position of the precursor benz[*a*]anthracene core, similarly to related angucycline compounds such as jadomycins (Tibrewal et al. 2012).

Although being mostly synthesized similarly to related angucyclines, gilvocarcins can also be formed via an unusual 21-carbon decaketide intermediate, as opposed to the usual C_{20} backbone. (Kharel, Pahari, Shepherd, et al. 2012) Several gilvocarcin pathway enzymes are homologous to those in related pathways, such as GilOIV, GilOI, and GilOII, which correspond to jadomycin pathway oxygenases JadF, JadH, and JadG, respectively.

Additionally, the *gil* pathway genes can be replaced by corresponding genes of the *jad* pathway when expressed in a heterologous host and maintain their function (Fan and Zhang 2018; Kharel et al. 2007). Similarly to jadomycins, gilvocarcin biosynthesis includes C2,3 and C4a,12b dehydration steps, oxygenation at C5 and C12, followed by a only partially characterized oxidative ring opening reaction cascade involving Baeyer-Villiger oxidation. (Kharel, Pahari, Shepherd, et al. 2012; Tibrewal et al. 2012). The reaction cascades of especially deletion mutant strains yield an abundance of biosynthetic shunt products, due to which the post-PKS biosynthetic steps and substrates have been difficult to characterize (Pahari, Kharel, Shepherd, van Lanen, et al. 2012). However, the oxygenase GilOII has been identified as the key enzyme involved in the C-C bond cleavage reaction. Similarly to the homologous enzyme JadG, GilOII is $FADH_2$-dependent. (Tibrewal et al. 2012) According to more recent studies, both GilOI and GilOII can be classified as antibiotic biosynthesis monooxygenases (Nuutila et al. 2024).

Kinamycins are diazafluorene compounds that belong to the family of B-ring modified non-classical angucyclines (X. Liu et al. 2018a). They share a lot of similarities to jadomycins and gilvocarcins but the final structure of kinamycins contain a contracted five-membered B-ring. The antimicrobial property of kinamycins A-D against Gram-positive bacteria was recognized upon their discovery in *S. murayamaensis* in 1970 (Ito et al. 1970). In addition, kinamycins A and C exhibit a significant anticancer effect, as both have shown to have a very potent cell growth inhibitory effect, possibly due to the reactive diazo group in their diazobenzo[*b*]fluorene scaffold (Hasinoff et al. 2006). Several analogues have been discovered since isolating the first kinamycins A-D, including intermediates and shunt products in the biosynthesis pathway. Unlike previously mentioned compound groups, kinamycins feature a five-membered B-ring and a diazo group. Despite the unique structure, kinamycin synthesis resembles that of jadomycins and gilvocarcins (Kharel, Pahari, Shepherd, et al. 2012)

The kinamycin producing biosynthetic pathway was first studied in *S. ambofaciens*, from which kinamycins A-D were originally isolated. However, a fully functional *kin* gene cluster could not be identified (Gould et al. 1998). The *alp* gene cluster was then isolated from *S. ambofaciens* ATCC 23877, which produces compounds called alpomycins, belonging to the kinamycin family of antibiotics. A mutation strain lacking a regulatory enzyme coding gene *tetR* was found to constitutively produce kinamycins (Bunet et al. 2011). Thus, the *alp* gene cluster has been used to study the biosynthesis of kinamycins.

Upon the discovery of the *alp* gene cluster, the Baeyer-Villiger oxygenase AlpJ and FAD-dependent monooxygenase AlpK were identified to be involved in the oxidative B-ring cleavage and the subsequent C-C bond formation yielding an intermediate referred to as hydroquinone-kinobscurinone (B. Wang et al. 2015). Later, the full kinamycin gene cluster was isolated from *S. galtieri* Sgt26, in which additional genes involving the late tailoring steps such as acetylation, were identified, as they were lacking in the previously discovered *alp* gene cluster in *S. ambofaciens*. The late tailoring steps are responsible, for example, for the conversion of kinamycin F to D. (X. Liu et al. 2018b) Kinamycins can also yield dimeric structures. Lomaiviticins are a group of dimeric polyketides that are closely related to kinamycins. Lomaiviticins A contains two diazofluorenes joined by a C-C bond, and it can be found in its monomeric form in kinamycin natural products (Kersten et al. 2013; B. Wang et al. 2015)

All kinamycin, gilvocarcin, and jadomycin biosyntheses involve a similar B-ring cleavage reaction but kinamycin pathway diverges from the other two in the follow-up ring contraction, as presented in figure 15. In addition, all pathways feature dehydrorabelomycin as an early intermediate. (B. Wang et al. 2015). Similarly to JadG and GilOII, AlpJ catalyses the ring-opening reactions on dehydrorabelomycin to yield a lactonized intermediate. The lactone is then hydrolyzed to result in an aldehyde/acid product with an open ring that can undergo various rearrangements to yield distinct products. (Pan et al. 2017). AlpJ is homologous to JadG and GilOII, whereas AlpK belongs to a subfamily of FAD-dependent monooxygenases that is not present in previously discussed pathways, suggesting a novel catalytic mechanism. It is likely closely associated with AlpJ in acting as a $FADH_2$ cofactor supplier. (B. Wang et al. 2015)

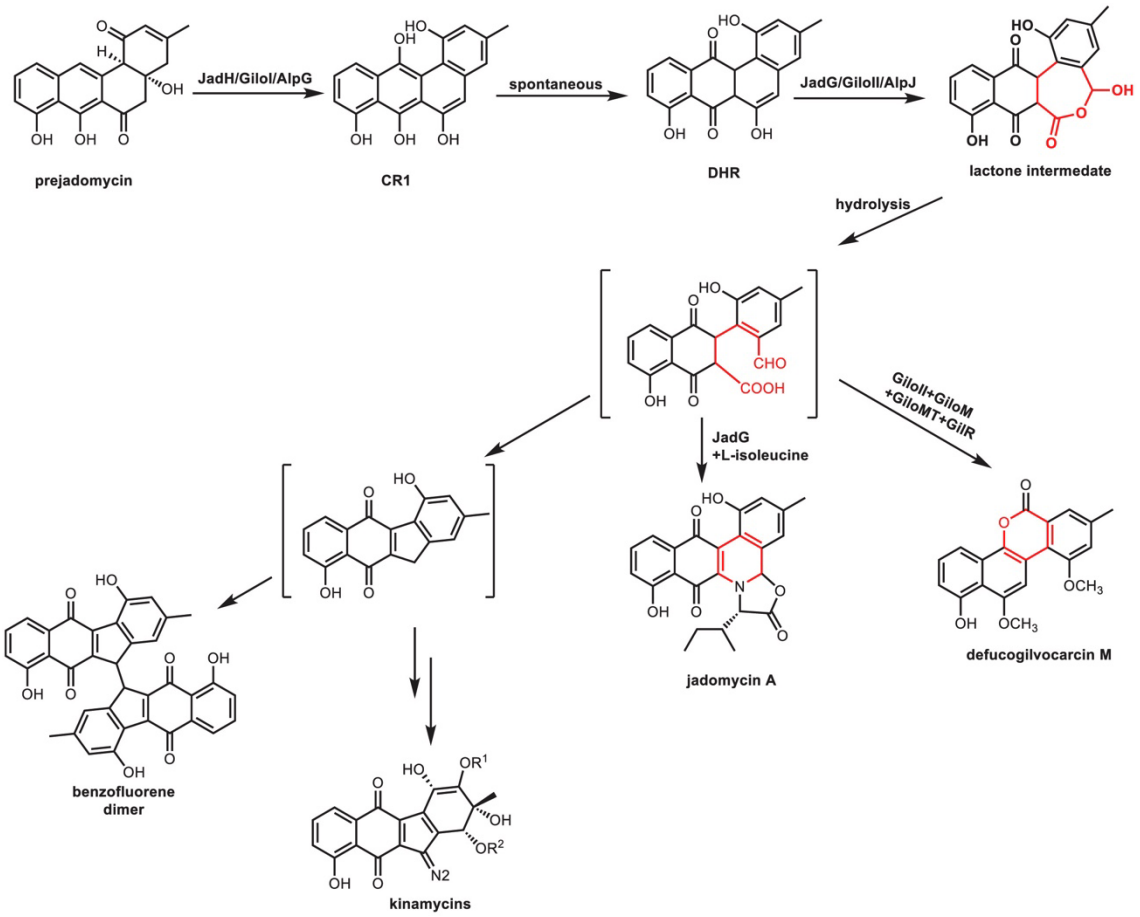

Figure 15. Kinamycin, jadomycin A, and defucogilvocarcin M biosynthetic pathways. All pathways share the initial steps, including the lactonized ring formation via JadG, GilOII, and AlpJ form prejadomycin.

It is well established that several non-classical angucyclines share similarities in both pathways in both early polyketide synthesis, as well as in the downstream tailoring processes. Baeyer-Villiger oxidation catalyzed by FAD-dependent monooxygenases plays a key role in the biosynthesis of multiple A- and B-ring cleaved compounds. (Tibrewal et al. 2012) The biosynthetic pathways of jadomycins, kinamycins, and gilvogarcins each require such an oxygenase, including JadG, GilOII, or AlpJ in the jadomycin, gilvocarcin, and kinamycin pathways (Fan and Zhang 2018; B. Wang et al. 2015). The jadomycin and gilvocarcin pathways also require an FAD/FMN reductase JadY or GilH that is not found in the kinamycin pathway, which rather features the unique AlpK. In addition, recent investigations into the kinamycin biosynthetic pathway have corroborated the long-postulated aldehyde/acid intermediate, shown in figure 16, which is likely shared in related pathways but only recently definitively confirmed (B. Wang et al. 2015). This intermediate is formed from dehydrorabelomycin and undergoes C-C bond cleavage to yield key lactonized intermediates, such as jadomycin A in the jadomycin

pathway, defuco-pregilvocarcin M in gilvocarcin pathway, and hydroquinone-kinobscurinone in the kinamycin pathway. The experimental verification of the aldehyde/acid intermediate further highlights the similarities between these pathways and sheds light on the ring-cleavage mechanism in B-ring modified structures. (Fan and Zhang 2018; Kharel, Pahari, Shepherd, et al. 2012; B. Wang et al. 2015).

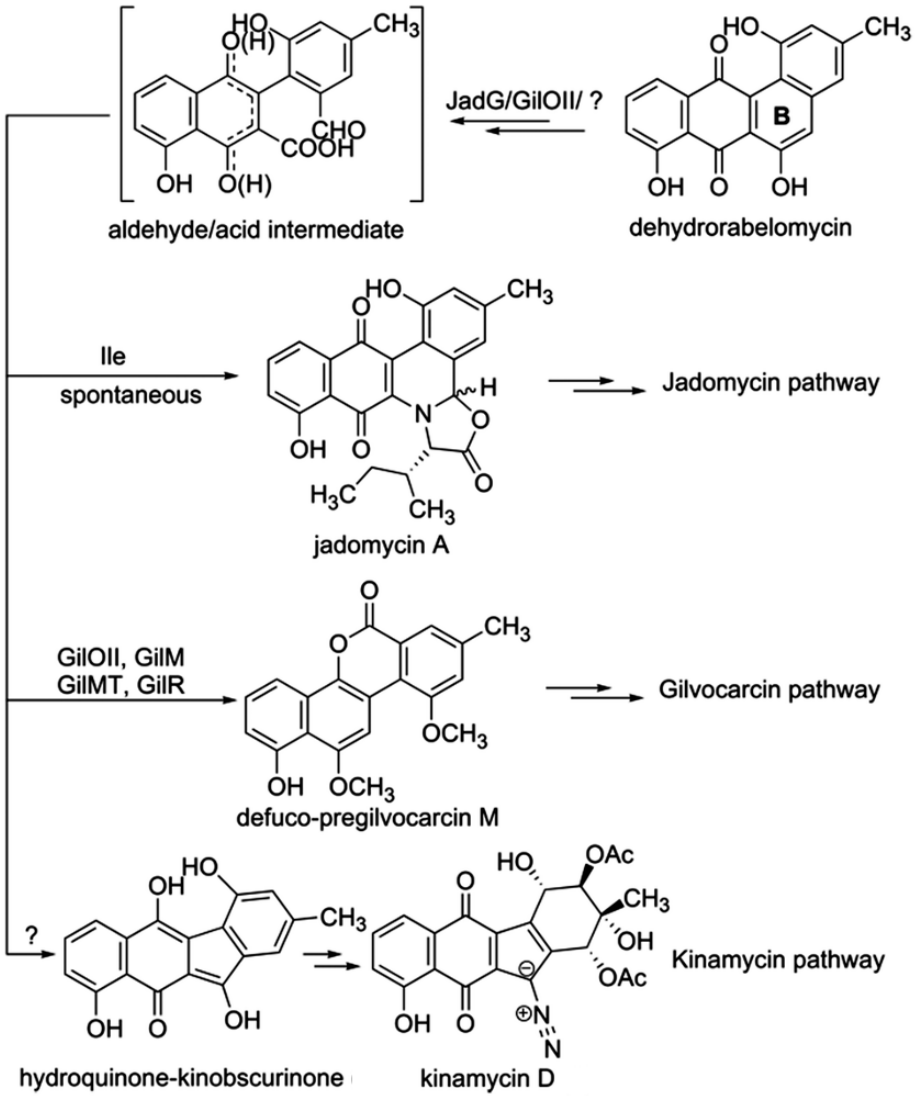

Figure 16. The aldehyde/acid intermediate. The Baeyer-Villiger oxidation results in the formation of an aldehyde/acid intermediate with an opened B-ring. The intermediate is then modified into various precursors in related pathways such as the jadomycin, gilvocarcin, and kinamycin pathway. Figure modified from Wang et al. 2015.

1.3.2.3. Angucyclines with rearrangements in the C-ring

Compared to many A- and B-ring modified structures, C-ring rearrangements are less frequent, and the mechanism of their biosynthesis is often poorly characterized (Elsayed et al. 2023). Several compounds featuring C-ring cleavage, for example fluostatin and lugdunomycin have, however, been identified. Unlike most non-classical angucyclines, many C-ring cleaved compounds have been discovered fairly recently (Nuutila et al. 2024). Other modifications such as C-ring expansion have also been reported (Ma et al. 2015). Similarly to several other classical and non-classical angucycline pathways, the C-ring cleaved angucycline compounds arise from UWM6, which undergoes C12-hydroxylation and 6-ketoreduction (Nuutila et al. 2024). After those common steps, the biosynthesis of C-ring cleaved compounds branches drastically, yielding biosynthesis pathways that are not often seen in other types of known angucyclines. Several pathway mechanisms have been suggested, and rarely fit the description for Baeyer-Villiger type oxidations that are proposed for several A- and B-ring cleaved structures. (Mikhaylov et al. 2021)

Fluostatins, classified as non-classical C-ring modified compounds, feature a fluorenone chromophore as well as an unusual skeleton with a contracted C-ring, as presented in figure 17 (C. Yang et al. 2015). Similarly to kinamycins and lomaiviticins, fluostatins belong to the family of benzofluorene-containing non-classical angucyclines (C. Yang et al. 2021) Fluostatins A and B were originally isolated from *Streptomyces* sp. TA-3391 in 1998, and their inhibitor activity against dipeptidyl peptidase III was recognized upon discovery (Akiyama et al. 1998). Since then, several analogues have been identified through methods such as natural isolation, heterologous expression of different gene clusters, and manipulation of the biosynthetic genes (C. Yang et al. 2021). Later, fluostatins were also recognized for their antitumor and antibacterial properties, and more recently efforts have been made to elucidate their complete biosynthesis. (Tohyama et al. 2025; C. Yang et al. 2015)

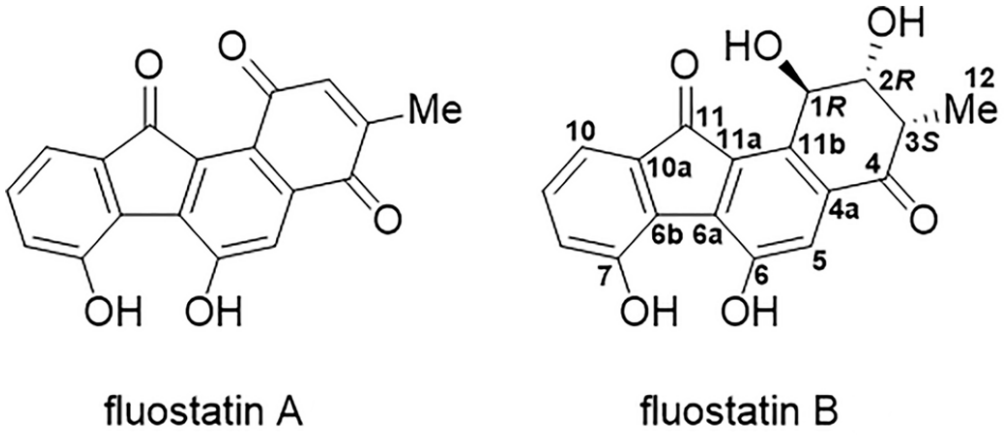

Figure 17. The structure of fluostatins A and B. Fluostatins feature a fluorenone chromophore as well as a contracted C-ring. Figure modified from Tohyama et al. 2025.

Being related to other benzo[*b*]fluorene-containing compound classes, the *fls* and *fluo* gene clusters encoding fluostatins share similarities and homologous enzymes with other known pathways, as illustrated in figure 18. The *fls* pathway was originally identified from *Micromonospora rosaria* SCSIO N160, in which the bifunctional oxygenase FlsO2 was characterized (Jin et al. 2018; C. Yang et al. 2015). Heterologous expression of the cluster in a *Streptomyces* host led to the discovery of novel intermediates fluostatin L and heterodimeric difluostatin A. FlsO2 is responsible for 4a/12b-dehydration, converting prejadomycin to dehydrorabelomycin via CR1, similarly to the antibiotic biosynthesis monooxygenase JadH (C. Yang et al. 2015). Following this step, the monooxygenase FlsG, homologous to AlpJ, catalyzes B-ring contraction to yield a benzofluorene intermediate. The oxygenase FlsO1 functions similarly to the unusual FAD-dependent monooxygenase AlpK, performing C5 hydroxylation on the contracted B-ring to form the common intermediate hydroquinone-kinobscurinone. (C. Yang et al. 2021)

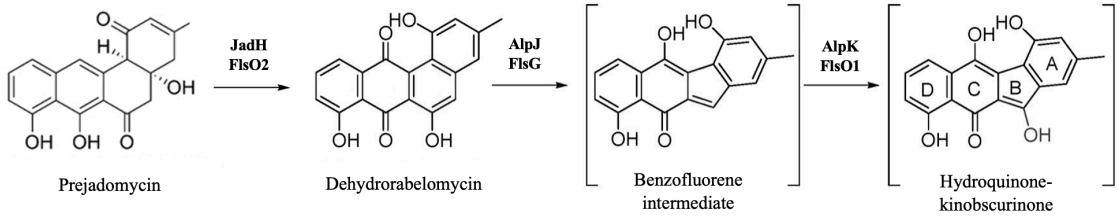

Figure 18. Early fluostatin tailoring steps. Prejadomycin is dehydrated by JadH homolog FlsO2 to dehydrorabelomycin, then converted via FlsG-catalyzed B-ring contraction into a benzofluorene intermediate. FlsO1 then hydroxylases C5 to yield hydroquinone-kinobscurinone. The subsequent steps remain poorly characterized. Figure modified from Yang et al. 2021.

The *fluo* gene cluster shares surprisingly little homology with the *fls* cluster regarding tailoring genes. Fluo5 and Fluo6 are also homologous to AlpK and AlpJ, respectively, and catalyze for similar reactions. (Jin et al. 2018) The hydroquinone-kinobscurinone intermediate appears in related pathways such as kinamycin biosynthesis, and comparative genomics has made it possible to identify the roles of the fluostatin pathway enzymes involved in its formation. Although several other fluostatin tailoring enzymes have been identified in the *fls* and *fluo* clusters, the subsequent steps leading to the fluorenone core assembly and C-ring contraction remain unknown. (Jin et al. 2018; Mikhaylov et al. 2021)

Lugdunomycin was isolated in 2019 from *Streptomyces* sp. QL37 upon research on cryptic biosynthetic gene clusters in *Streptomyces*. After its discovery, it has gained attention due to its unique structural properties and antibiotic activity, and it has been proposed that lugdunomycin may represent a novel subclass of aromatic polyketides. (Wu et al. 2019) Lugdunomycin expands the structural diversity of angucyclines, guiding the research into an exciting direction.

Lugdunomycin contains a structure unseen in known angucycline compounds (Vysloužilová and Kováč 2024). It is composed of a heptacyclic ring structure with a spiroatom, a benzaza[4,3,3]propellane moiety, and two carbon stereocenters, and the structure is presented in figures 7 and 17 (Wu et al. 2019). Similarly to other non-classical angucyclines, the lugdunomycin *lug* gene cluster encodes for a series of post-PKS tailoring enzymes, such as reductases, oxygenases, and group transferases, as well as regulator and transporter proteins. The full details of the lugdunomycin biosynthetic pathway are still to be fully characterized, although a rare mechanism of structure

extension by a Diels-Alder reaction has been proposed as the final step (Mikhaylov et al. 2021; Wu et al. 2019). The biosynthesis begins, however, similarly to well-known classical angucyclines in producing UWM6 by minPKS enzymes LugA-F. The minimal PKS, as well as some tailoring enzymes, contain homologs in related gene clusters *pga*, *urd*, and *lan* (Nuutila et al. 2024). In early post-PKS tailoring, UWM6 is converted into rabelomycin and tetrangomycin, and their 8-*O*-methylated forms. The conversion into rabelomycin and 8-*O*-rabelomycin represents a shunt pathway, whereas 8-*O*-methyltetrangomycin can be further modified into lugdunomycin via a Baeyer-Villiger oxidation in C6a-C7 bond of ring C, making it a key intermediate in the pathway. (Xiao et al. 2020)

The main steps of the biosynthesis of lugdunomycin are catalyzed by four oxygenases LugOI-OII and LugOV, of which LugOI and LugOII cluster closely with related pathways in comparative genome analyses (Elsayed et al. 2023). LugOI catalyzes C12 hydroxylation similarly to well-known flavoprotein monooxygenases including PgaE, UrdE, and LanE, yielding 12-hydroxy-UWM6 (Nuutila et al. 2024; Xiao et al. 2020). A fusion protein LugOII is homologous to PgaM and UrdM, and responsible for 2,3-dehydration and C6 ketoreduction on 12-hydroxy-UWM6. Based on *in vitro* studies, however, LugOII is known to carry an additional function in C1 ketoreduction, unlike its related enzymes, resulting in the formation of tetrangomycin (Xiao et al. 2020). The SDR domain of LugOII, LugOIIred, is orthologous to LanV sharing similar substrate specificity and catalytic activity (Nuutila et al. 2024; Paananen et al. 2013). After further tailoring by enzymes such as the methyltransferase LugN, two more oxygenases LugOIII and LugOV are involved. No close homologs of these oxygenases have been identified in other angucycline biosynthetic clusters. Both LugOIII and LugOV are antibiotic biosynthesis monooxygenases that catalyze the C-ring cleavage in the lugdunomycin pathway. (Elsayed et al. 2023)

LugN is a SAM-dependent *O*-methyltransferase responsible for the formation of presumably crucial lugdunomycin intermediates. The activity of LugN results in the formation of 8-*O*-methyltetrangomycin. However, the *O*-methylation at C8 via LugN is not dependent on the C6 ketoreduction, unlike the C12 hydroxylation. Therefore, the C6 ketoreduction and 8-*O*-methylation steps may occur in any order. The shunt product rabelomycin is methylated into 8-*O*-methylrabelomycin correspondingly. LugG, a 7-ketoreductase, will guide the pathway forward by forming 7-deoxo-7-hydroxy-8-*O*-

methyltetrangomycin in the presence of NADPH. (Nuutila et al. 2024) The formation of all C-ring cleaved angucyclines are likely to contain an epoxide intermediate with both C7 and 12 keto-groups reduced. LugOIII is proposed to be responsible for the C6a-C12a epoxidation step, while LugOV is associated with the breakage of the C-ring. The specific function of LugOV, however, is still not clear. It is known that it acts preferably on 8-methoxy-containing intermediates, whereas LugOIII can use both methylated and non-methylated intermediates as a substrate. (Elsayed et al. 2023) After C-ring cleavage, the lugdunomycin synthesis is proposed to end in Diels-Alder reaction that yields the benzaza[4,3,3]propellane skeleton with the [4+2] cycloaddition reagents provided by related biosynthetic pathways. The intermediates in these pathways undergo oxidative cleavage and dehydration to yield maleimycin and hydroxy-*o*-quinone, respectively, which are combined to form a six-membered cyclic product that is then fused into the open C-ring scaffold yielding a novel fused ring system. (Wu et al. 2019) The early tailoring steps of the lugdunomycin pathway are shown in figure 19.

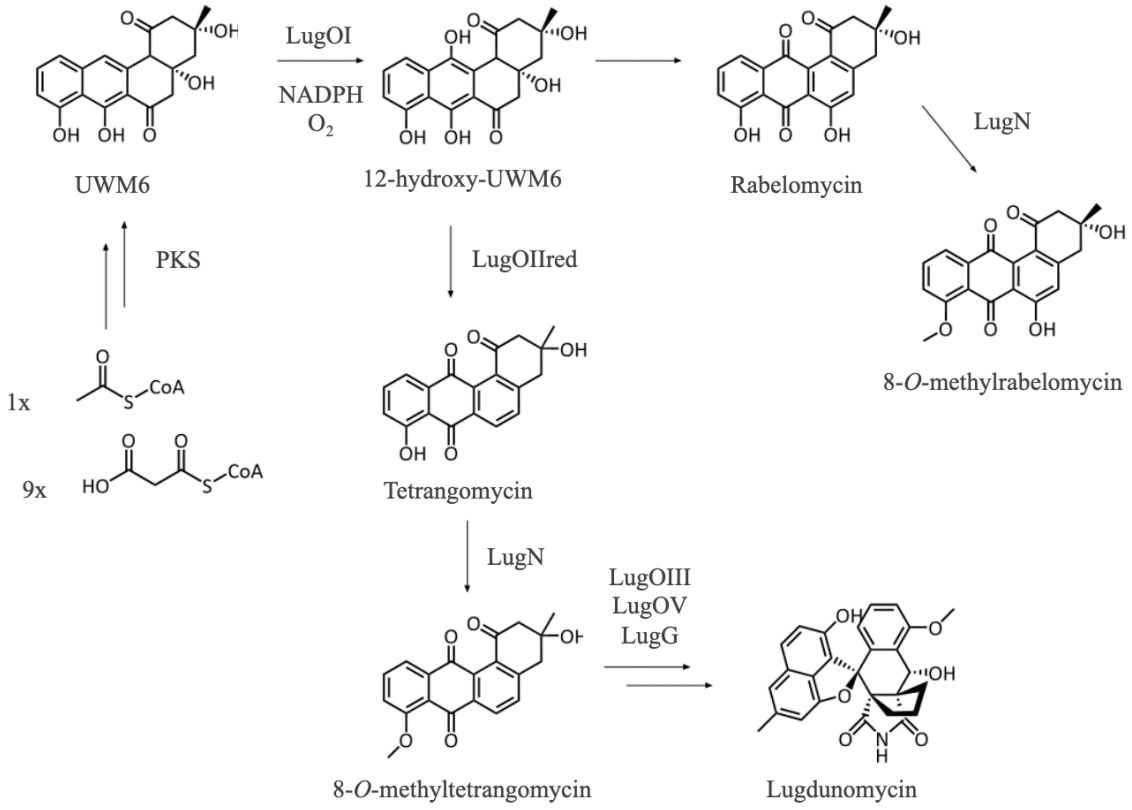

Figure 19. Early tailoring steps on the lugdunomycin pathway. Tetrangomycin and 8-*O*-methyltetrangomycin are produced from UWM6 via LugOI, LugOIIred, and LugN. These intermediates are then converted into lugdunomycin with complex reaction requiring a C-C bond breakage that are catalyzed by oxygenases and reductases such as LugOIII, LugOV, and LugG.

Overall, the study of angucyclines highlights how small variations in biosynthetic pathways can generate remarkable structural diversity with significant biological potential, as is illustrated in figure 20. Majority of the known classical and non-classical angucycline compounds arise from shared intermediates, and continued investigations of these pathways allow new insights into natural product chemistry and drug discovery. Lugdunomycin is a recent and intriguing example of such discoveries, as it provides new opportunities for expanding polyketide diversity and guides the search for novel antimicrobial compounds.

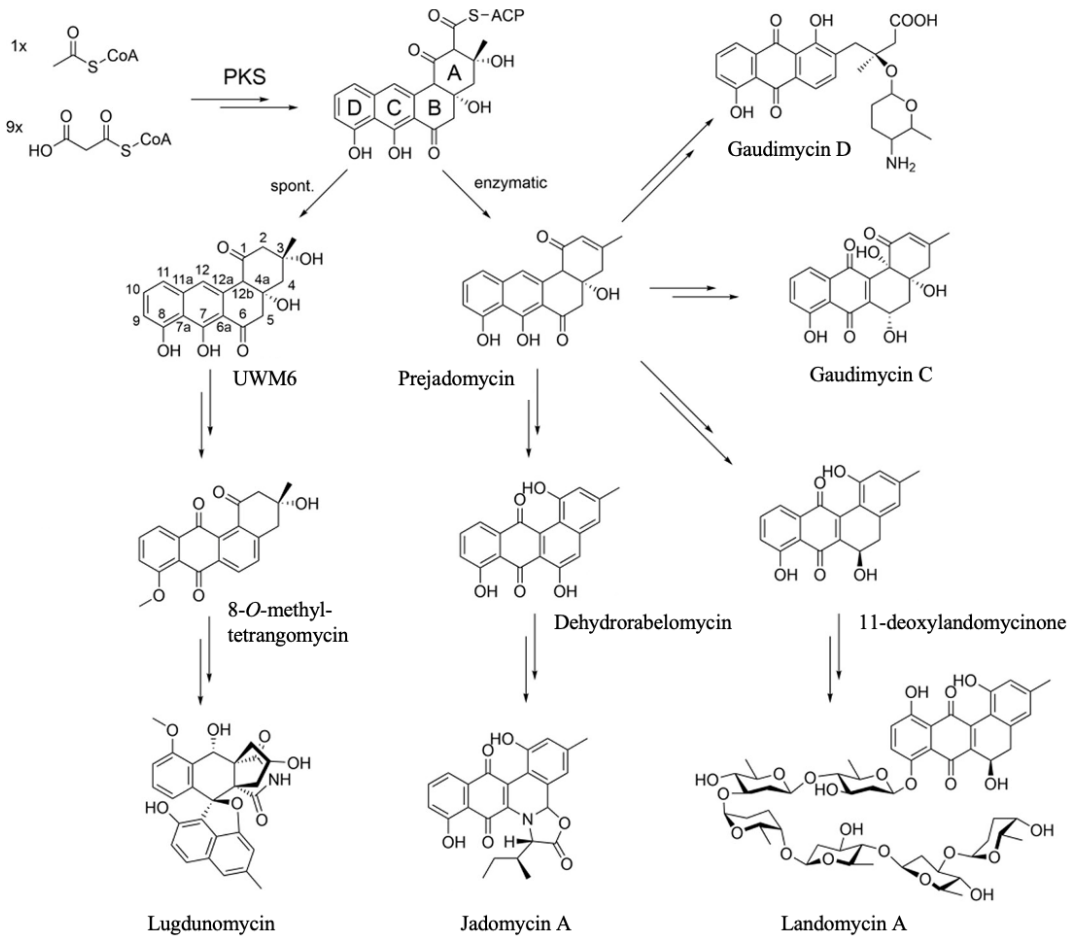

Figure 20. Diversification of angucycline antibiotics. The pathways leading to both classical and non-classical angucyclines share key intermediates such as UWM6 and prejadomycin that undergo modifications to yield a huge variety of structures with intriguing biological activities. Figure modified from Nuutila et al. 2024.

1.4 BioBricks design principles

Reconstructing and modifying biosynthetic gene clusters in heterologous hosts require precise synthetic biology assembly mechanisms. BioBricks is a standardized system developed in the early 2000s for assembling synthetic genetic elements by recycling the

same restriction nucleases in iterative reactions (Knight, Tom 2003). It was created to provide a reliable, simple, and efficient method for constructing genetic constructs, such as bacterial expression systems. In BioBricks, each genetic fragment represents a BioBrick that can be joined into another BioBrick through digestion and ligation, therefore yielding a two-fragment genetic construct now called a single BioBrick. (R. P. Shetty et al. 2008) This is based on the standardized prefix and suffix that flank each BioBrick and contain restriction nucleases that cleave the DNA double helices at specific sites. The prefix, sitting at the 5' end of the BioBrick, contains restriction sites for *EcoRI* and *XbaI*, while the suffix at the 3' end includes restriction sites for *SpeI*, also known as *BcuI*, and *PstI*. Therefore, these recognition sites cannot be present within the genetic fragment itself. (Knight, Tom n.d.; R. Shetty et al. 2011; R. P. Shetty et al. 2008)

To join two BioBricks together, the first BioBrick is digested with *SpeI* and the second with *XbaI*, resulting in cleavage at the *SpeI* restriction site at the 3' end of the first BioBrick, and at the *XbaI* restriction site at the 5' end of the second BioBrick, as shown in figure 21. The ligation of these two sites results in a "scar-site" that cannot be digested with either of the two enzymes (Knight, Tom 2003). Thus, joining two BioBricks together will result in the formation of a single BioBrick. The resulting BioBrick is flanked by a *EcoRI* and *XbaI* restriction sites at the 5' end, and *SpeI* and *PstI* sites at the 3' end. This allows adding further genes proceeding or following the resulting BioBrick through subsequent digestion and ligation steps. (R. Shetty et al. 2011) Each of the plasmid constructs that were assembled with BioBricks and used in this study contained a resistance cassette, such as an ampicillin resistance marker, to identify clones with the correct assemblies after transformation into *E. coli*.

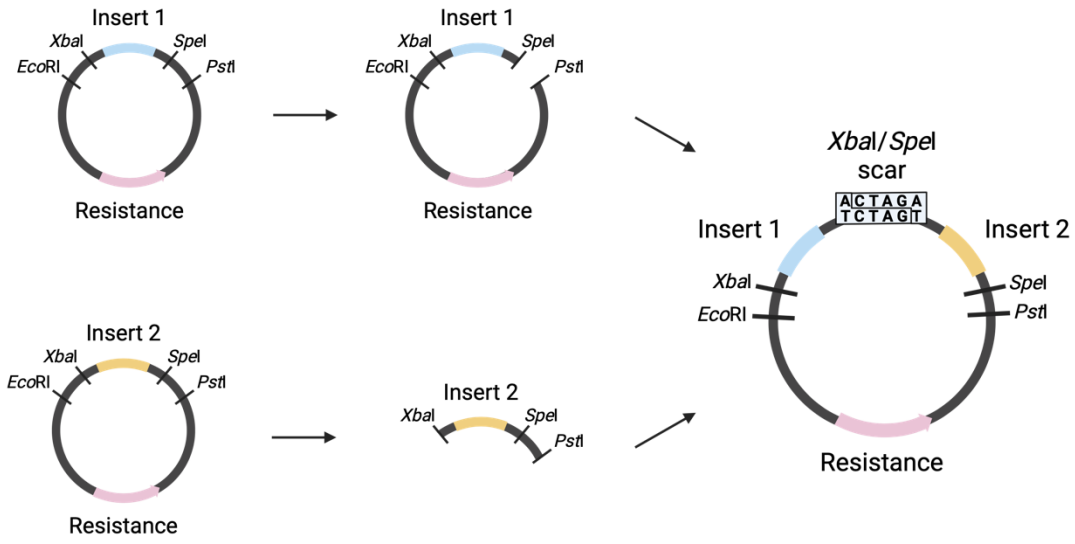

Figure 21. BioBricks assembly principle. The vector and insert are digested with restriction enzymes XbaI and PstI, and SpeI and PstI, respectively, to yield a new genetic construct containing a scar site that cannot be re-digested with the same set of restriction enzymes, while the operon remains flanked by BioBricks-enzyme recognition sites to allow further editing.

Additional genetic elements were inserted into the plasmid construct by either a two-way or three-way assembly mechanism. In the two-way assembly, the plasmid backbone was digested with *SpeI* and *XbaI*, and the insert with *XbaI* and *PstI*. In some cases, the three-way assembly was used to combine two inserts into a backbone by digesting the upstream element with *EcoRI* and *SpeI*, and the downstream element with *XbaI* and *PstI*. In this case, the backbone was digested with *EcoRI* and *PstI*.

BioBricks was used in this study due to not only its simplicity and efficiency, but also its suitability when building a genetic library. BioBricks is a modular system that allows reuse of standardized genetic parts in multiple constructs without further modifications by using the same four restriction enzymes.

2 Aims of the study

1) Establish a synthetic biology platform to for production of angucycline-type natural products in *Streptomyces*
2) Develop genetic tools for precise gene expression in *Streptomyces*
3) Assemble tailoring steps of the lugdunomycin biosynthetic pathway
4) Detect and analyse lugdunomycin pathway intermediates as a part of pathway validation and optimization

3 Materials and methods

3.1 Assembling plasmid constructs with BioBricks in *E. coli* TOP10

3.1.1 Expression construct design

The sequences of the genes *lugOI*, *lugOII*$_{red}$, *lanV*, and *lugN* in pUC57, as well as the synthetic promoters SP5, SP11, SP15, and SP44 in pUC-KAN-GW, were designed with Benchling to be compatible with BioBricks and ordered from Genewiz (Azenta Life Sciences). The ordered genes were flanked by the BioBricks prefix (AATTCGCGGCCGCTTCTAGAG) and suffix (TACTAGTAGCGGCCGCTGCAG), containing restriction sites for *EcoRI*, *XbaI*, and *SpeI* (*BcuI*), *PstI*, respectively. The sequences also contained an RBS sequence (AGGAGC, AGGAGG or AGGAGA) upstream of the gene.

The BioBricks-compatible plasmid backbones pSB1A3-J04450, pSB1C3-J04450, and pSB1K3-J04450 with resistance cassettes for ampicillin, chloramphenicol, and kanamycin, respectively, were used in constructing most of the plasmids. In some cases, other compatible plasmids, mainly pUC57, were used.

3.1.2 Expression construct assembly

The plasmid backbones pSB1A3-J04450, pSB1C3-J04450, and pSB1K3-J04450 were first digested with *EcoRI* and *PstI* FastDigest Restriction enzymes from Thermo Fisher Scientific in FastDigest Green Buffer from Thermo Fisher Scientific according to manufacturer's instructions. The BioBricks-compatible genetic fragments to be inserted were similarly digested with *EcoRI* and *PstI*. FastAP Thermosensitive Alkaline Phosphatase (1 U/µl) by Thermo Fisher Scientific was used in the digestion reaction according to manufacturer's instructions to prevent re-ligation of the digested fragments. To confirm the size of the digested gene fragment, or when a non-BioBricks-compatible plasmid backbone, such as pUC57 was used in the assembly, fragments were run on an 1 % agarose gel in TAE buffer (40 nM Tris base, 20 mM acetic acid, 1 mM EDTA) at 90 V with Midori Green Advance DNA stain from Nippon Genetics. The gene fragments were purified from the gel with the GeneJET Gel Extraction Kit from Thermo Fisher Scientific according to the instructions from the manufacturer. The digested gene

fragments were ligated with Thermo Fisher Scientific T4 ligase (5 U/µl) in T4 Ligase Buffer according to manufacturer's instructions.

When adding genetic elements prior to the first gene in the cassette, the backbone was digested with *EcoRI* and *SpeI*, and the insert with *EcoRI* and *XbaI*. When the expression constructs were finished, the assembly-backbone was replaced with pSET152 for bacterial conjugation by digesting both the insert and the backbone with *EcoRI* and *PstI*, as described previously.

3.1.3 Transformation into *E. coli* TOP10

To prepare competent *E. coli* TOP10 and ET12567/pUZ8002 cells, a single colony was inoculated into 2x YT (1,6 % w/v tryptone, 1 % w/v yeast extract, 0,5 % w/v NaCl) and grown overnight at 37 °C in 250 rpm shaker without antibiotics (TOP10), or with 25 µg/ml chloramphenicol and kanamycin (ET12567/pUZ8002). The overnight culture was diluted into 100 ml 2x YT and grown until OD_{600} reached approximately 0,5. The culture was cooled on ice for 10 minutes, after which the cells were collected by centrifugation at 1000 x g at 4 °C for 10 minutes. The cell pellet was gently washed with 10 ml of cold 50 mM $CaCl_2$ and incubated on ice for 10 minutes. The cells were centrifuged, after which the pellet was washed and incubated on ice as previously and centrifuged again. The pellet was then resuspended in 2 ml of cold 0,05 mM $CaCl_2$ with 15 % glycerol and aliquoted for storage in -80 °C.

The assembled plasmid constructs were transformed into *E. coli* TOP10 after ligation by mixing 10 µl ligation mixture with 50 µl competent *E. coli* TOP10 cells. The mixture was then incubated on ice for 5 minutes, heat-shocked at 42 °C for 60 seconds and incubated on ice for 15 minutes. After incubation, 1 ml of 2x YT media was added, and the cells were cultivated at 37 °C in a shaker with a rotation speed of 250 rpm for 60 minutes. Approximately 100 µl of the cells were plated on LA (10 g/l tryptone, 5 g/l yeast extract, 10 g/l NaCl, 15 g/l agar with 100 µg/ml ampicillin, 50 µg/ml kanamycin or 20 µg/ml chloramphenicol) selection plates and grown overnight at 37 °C. Liquid precultures were started from the transformation plates the following day in 6 ml LB (10 g/l tryptone, 5 g/l yeast extract, 5 g/l NaCl) with antibiotics and grown in 37 °C in 250 rpm shaking overnight. The plasmids were extracted from the cultures with GeneJET Plasmid Miniprep Kit from Thermo Fisher Scientific according to the instructions from the

manufacturer and the concentration measured with Thermo Fisher Scientific NanoDrop One UV-Vis spectrophotometer. The final assemblies with the pSET152 backbone were transformed into *E. coli* ET1 cells in a similar manner for conjugation.

3.2 Construction of the *S. coelicolor* M1152Δ*matAB*/pMC6BD -host strain

3.2.1 pMC6BD plasmid extraction from *S. lividans* TK24

To extract and transform the pMC6BD plasmid into the new host strain, the old strain *S. lividans* TK24 containing the plasmid was grown in TSB (CM129 tryptone soya broth, OXOID) with 50 µg/ml thiostrepton at 30 °C with shaking at 300 rpm for 7 days. The culture was centrifuged at 4500 x g for 10 minutes. The resulting cell pellet was resuspended in a solution with 4 mg of lysozyme (2 mg/ml lysozyme in 0,3 M sucrose, 25 mM Tris, pH 8.0, 25 mM EDTA, pH 8.0) and incubated at 37 °C for 30 minutes.

For lysing the cells, the solution was vigorously mixed, 1 ml alkaline SDS solution (0,3 M NaOH, 2 % SDS) was added, and mixed. The solution was incubated at 55 °C for 20 minutes with a loosely capped tube, then vigorously mixed again, and allowed to cool to room temperature. After cooling, 500 µl acid phenol/chloroform (1:1 mixture of phenol, pH 5.0, and chloroform) was added. The mixture was thoroughly vortexed and centrifuged at 4500 x g for 10 minutes at room temperature. The upper aqueous phase was carefully transferred to a new tube, and 1 ml of chloroform was added. The solution was vortexed vigorously, centrifuged again as previously, and the upper phase transferred to a new tube.

To precipitate the DNA, 250 µl of 3 M unbuffered sodium acetate was added to the aqueous phase, the solution mixed, and 2,5 ml isopropanol added. The mixture was incubated at room temperature for 15 minutes and centrifuged at 4500 x g for 15 minutes. The DNA pellet was washed with 3 ml of 70 % ethanol, centrifuged, and air-dried under vacuum. The dried pellet was then resuspended in 100 µl TE buffer (10 mM Tris-HCl, pH 8.0, 1 mM EDTA, pH 8.0). 1 µl of Rnase A (1 mg/ml) was added and the solution incubated at 37 °C for 45 minutes. The DNA concentration was quantified using NanoDrop.

3.2.2 Preparing *S. coelicolor* protoplasts

S. coelicolor M1152Δ*matAB* spores were cultivated in 50 ml YEME (3 g yeast extract, 5 g peptone, 3 g malt extract, 10 g glucose, 340 g ultra-pure sucrose in 1 l distilled water) and grown in a shaker rotating at 300 rpm at 30 °C for 3 days. The culture was centrifuged at 1500 x g for 10 minutes, and the pellet washed twice with 5 ml 10,3 % sucrose. A P buffer solution was prepared by dissolving 51,5 g of sucrose, 0,125 g of K_2SO_4, and 1,01 g of $MgCl_2 \cdot 6\ H_2O$ in 400 ml of distilled water forming a P buffer. To create the final P+ buffer solution, 0,5 % KH_2PO_4, 3,68 % $CaCl_2 \cdot 2\ H_2O$, 5,73 % TES buffer, pH 7.2, and 200 µl of trace element solution (40 mg $ZnCl_2$, 200 mg $FeCl_3 \cdot 6\ H_2O$, 10 mg $CuCl_2 \cdot 2\ H_2O$, 10 mg $MnCl_2 \cdot 4\ H_2O$, 10 mg $Na_2B_4O_7 \cdot 10\ H_2O$, 10 mg $(NH_4)_6Mo_7O_{24} \cdot 4\ H_2O$ in 1 l distilled water) were added to 80 ml of the P buffer solution. An 8 mg lysozyme solution (2 mg/ml lysozyme in P+ buffer) was used to carefully resuspend the cell pellet containing the mycelium and incubated at 30 °C for 30 minutes. The formation of protoplasts was checked under the microscope, after which the solution was carefully mixed by pipetting three times and incubated further for 5-30 minutes. After the incubation, 4 ml of P+ buffer was added to the protoplast solution, the solution mixed gently and filtered. The protoplasts were sedimented by centrifugation at 1500 x g for 7 minutes, after which the pellet was suspended in 2-5 ml of P+ buffer and the solution aliquoted for storage. The protoplasts were first stored in -20 °C and moved to -80 °C after 24 hours.

3.2.3 Introducing pMC6BD into *S. coelicolor* protoplasts

The thawed *S. coelicolor* M1152Δ*matAB* protoplasts were centrifuged at 1500 x g for 7 minutes, the supernatant poured off and the pellet resuspended to the remaining supernatant, after which 20 µl of pMC6BD plasmid DNA was added and the solution mixed. 500 µl of 25 % PEG 4000 in P+ solution was added and mixed gently, after which the protoplast suspension was spread on R2YE plates and grown at 30 °C. After 1-2 days, when weak growth could be seen, 50 µg/ml thiostrepton was added to the plates and incubated further.

The plates were grown for 5 days, after which single colonies were streaked onto MS agar plates (20 g agar, 20 g mannitol, 20 g soya flour) with 50 µg/ml thiostrepton and incubated at 30 °C. After 5 days, the bacterial growth was scraped off into 30 ml E1 media (20 g glucose, 20 g starch, 5 g Farmamedia, 2,5 g yeast extract, 1,3 g $K_2HPO_4 \cdot 3\ H_2O$, 1 g $MgSO_4 \cdot 7\ H_2O$, 3 g NaCl, 3 g $CaCO_3$) with 0,2 g/ml adsorbent SEPLITE LXA1180

(SUNRESIN) polymeric resin and 50 µg/ml thiostrepton. The cultures were grown in 300 rpm shaking at 30 °C for 5 days.

3.3 Bacterial conjugation of recombinant plasmids into *Streptomyces* host

3.3.1 Preparation of *S. coelicolor* M1152Δ*matAB*/pMC6BD spores

The pMC6BD plasmid containing *S. coelicolor* M1152Δ*matAB* strains were grown on MS agar plates with 50 µg/ml thiostrepton at 30 °C for approximately 5 days until sufficient mycelial growth could be seen. The mycelium was harvested by adding 5 ml of sterile water on top of the plate, and the surface was carefully scraped to release the mycelium into a spore suspension. The suspension was vortexed vigorously for a few minutes to break the spore chains and filtered through a sterilized syringe with cotton wool. The filtered solution centrifuged at 4000 x g for 10 minutes to pellet the spores. The pellet was resuspended in 2 ml of sterile 40 % glycerol and aliquoted for storage at -80 °C.

3.3.2 Conjugation from *E. coli* into *S. coelicolor*

The *E. coli* ET12567/pUZ8002 cells transformed with the recombinant plasmids were used for conjugation into *S. coelicolor* M1152Δ*matAB* spores. The *E. coli* ET12567/pUZ8002 was inoculated into 10 ml LB with 25 µg/ml chloramphenicol, 25 µg/ml kanamycin, and 50 µg/ml apramycin and grown overnight. The culture was diluted 1:50 in fresh LB with antibiotic selection and grown until OD_{600} was approximately 0,5.

The grown cells were washed twice with LB to remove any antibiotic residue and resuspended in 5 ml LB. Roughly 10^8 *S. coelicolor* M1152Δ*matAB* spores were added to 500 µl 2x YT media, heat shocked at 50 °C for 10 minutes, then allowed to cool. *E. coli* cells were added to the heat-shocked spores and mixed. Most of the supernatant was poured off and the pellet resuspended in the remaining liquid, that was plated on MS agar with 10 mM $MgCl_2$. The plates were incubated at 30 °C for 16-20 hours, after which 0,5 mg nalidixic acid, 0,5 mg kanamycin, 0,5 mg chloramphenicol, and 1 mg apramycin were added.

After 5-7 days, when sufficient growth could be seen, single colonies were spread onto secondary MS agar plates with 0,5 mg kanamycin, 0,5 mg chloramphenicol and 1 mg

apramycin. The secondary plates were again grown at 30 °C for 7 days, after which the growth was scraped off into a liquid culture media.

3.3.3 *Streptomyces* culture and extraction of metabolites

The *Streptomyces* strains were pre-cultured in 30 ml TSB or SG media with 25 µg/ml chloramphenicol, 25 µg/ml kanamycin, and 50 µg/ml apramycin in 300 rpm shaking at 30 °C for 5 days until noticeable growth could be seen. The main cultures were grown in total volume of 50 ml containing SG, E1, or MS media with 5 ml of pre-culture and 5 ml of an adsorbent LXA1180 resin. The resin was added to the main cultures on the first day or after approximately 3-4 days. The main cultures were similarly grown in 300 rpm shaking at 30 °C for 6-8 days.

After culturing the strains, the produced metabolites were eluted from the resin. The resin was first separated from the cells by rinsing, after which excess water was removed, and the resin soaked in methanol in light shaking for approximately 1-2 hours to extract the compounds. The methanol was then cleared by either filtration or centrifugation.

3.4 UHPLC-analysis

The samples along with known standards were prepared and analysed on UHPLC with an UV-Vis detector for compound identification. The analysis was carried out with Shimadzu Nexera X3 system with a photodiode array detector and either a Kinetex C18 1.7 µm, 100 Å, 100 x 2.1 mm, Phenomenex) or a Kinetex phenyl-hexyl column (2.6 µm, 100 Å, 150 x 4.6 mm, Phenomenex). The program used 100 % ACN and 15 % ACN with 0,1 % formic acid.

3.5 Language revision

ChatGPT (OpenAI) was used for language editing and text polishing for selected parts of this thesis. All interpretation of scientific content and conclusions were produced by the author.

4 Results and discussion

Despite extensive efforts, biosynthesis of lugdunomycin (**1**), and other C-ring cleaved angucyclinones, is still poorly understood. (Elsayed et al. 2023) The importance of researching the formation of such novel compounds is, however, recognized. To elucidate the biosynthetic pathway, I initiated the study by cloning early genes required for production of a key angucycline pathway intermediate UWM6 (**2**) in our heterologous *Streptomyces* chassis. Second, I extended the pathway by inducing tailoring genes from the lugdunomycin pathway to produce the key products in early tailoring steps, which would facilitate enzymological studies for determining the role of the molecule in the C-ring cleavage of **1**. The structures of the key angucyclines discussed in this study are shown in figure 20.

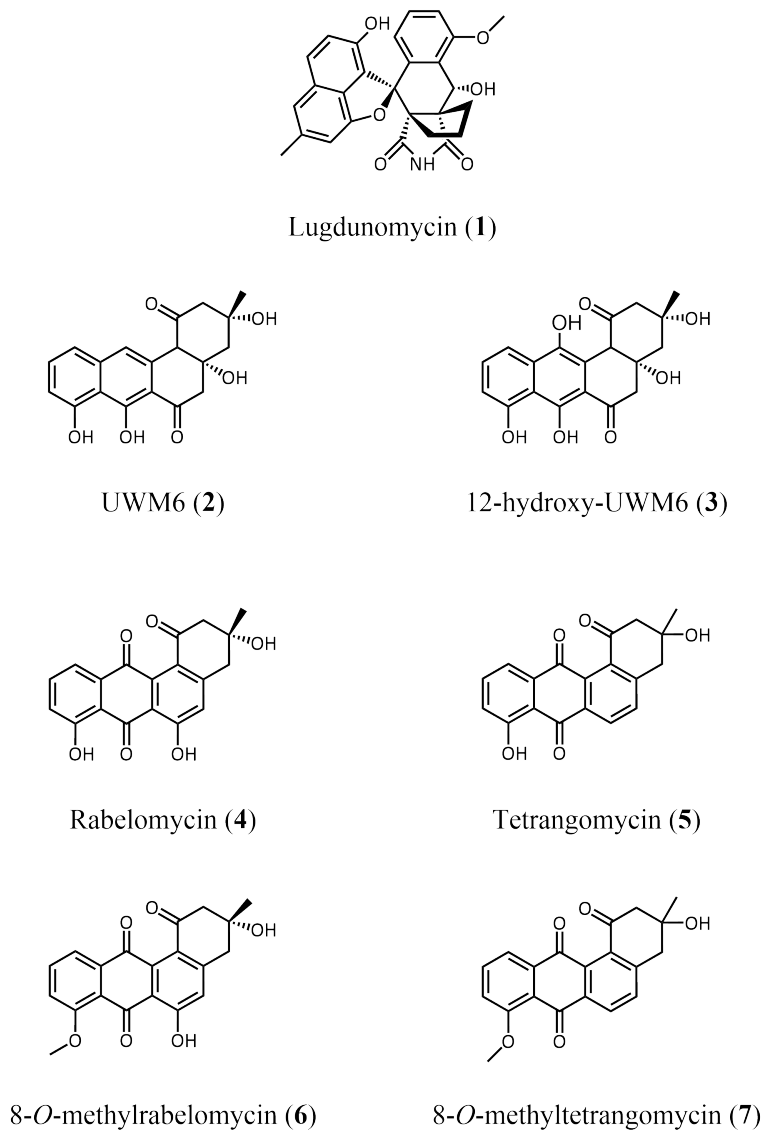

Figure 22. Angucycline structures discussed in this study.

This study was conducted according to the "Design-Build-Test-Learn" principles of synthetic biology, which is widely used in the field to create, guide, and optimize biological systems (Junyang Wang et al. 2021). First, the genetic constructs were designed to be compatible with the standardized BioBricks systems, and genes chosen based on earlier data. In the second phase, the constructs were assembled as described previously with BioBricks in *E. coli*. Next, the constructs were cloned into *S. coelicolor* and the recombinant strains grown for production of angucyclines. After analysis of samples by HPLC, the results were gathered and compared to expected outcomes to facilitate the design of subsequent development rounds.

4.1 Production of compound 2 in *S. coelicolor*

S. coelicolor M1152Δ*matAB* was used as the host strain, to which the engineered plasmids were introduced via bacterial conjugation. This strain is characterized by reduced mycelial aggregation due to alterations in the *matAB* gene cluster, making it particularly well-suited for metabolic engineering of polyketide pathways (Wang et al. 2022).

Previous work (Palmu et al. 2007) has resulted in the construction of the plasmid pMC6BD, which encodes early genes for formation of angucycline carbon scaffold, including the minimal PKS complex, a C9 ketoreductase, an aromatase, and a cyclase, all of which contribute to the formation of the first stable intermediate **2**. The minPKS complex contains genes responsible for the early pathway iterative Claisen condensation reaction utilizing the starter and nine extender units, thus forming the polyketide chain, as well as an acyl carrier protein that tethers the growing polyketide chain. In the pMC6BD plasmid, the long polyketide chain first formed by the minPKS complex is reduced by *snoaD*, following the aromatization of the first ring by *pgaL*, and eventually the polyaromatic structure of **2** is achieved by *pgaF* (Kallio et al. 2011; Palmu et al. 2007). The genes expressed in pMC6BD are shown in table 1.

Plasmid	Genes			
	minPKS	**KR**	**ARO**	**CYC**
pMC6BD	*snoa123*	*snoaD*	*pgaL*	*pgaF*

	OH	**KR**	**MT**
pSA001	*lugOI*		
pSA002	*lugOI*	*lugOIIred*	
pSA003	*lugOI*	*lanV*	
pSA004	*lugOI*		*lugN*
pSA005	*lugOI*	*lugOIIred*	*lugN*
pSA006	*lugOI*	*lanV*	*lugN*
pSA007	*lugOI*	*lugOIIred*	*lugN*
pSA008	*lugOI*	*lugOIIred*	*lugN*
pSA009	*lugOI*	*lugOIIred*	*lugN*

Table 1. Plasmids used in this study. The pMC6BD plasmid was obtained from previous research by Palmu et al. 2007. Plasmids pSA001-009 were constructed in this study by using BioBricks.

However, the pMC6BD plasmid was earlier cloned to another heterologous host, *S. lividans* TK24, which has been problematic for studying angucycline biosynthesis as endogenous genes have been noted to interfere with product formation (Palmu et al. 2007). To ensure a successful platform for studying **1** biosynthesis, the pMC6BD plasmid was introduced into a new host strain *S. coelicolor* M1152Δ*matAB* via protoplast transformation. The recombinant strain was cultivated and the production profile analyzed on UV-Vis UHPLC. **2** was successfully produced in high yields without

undesired byproducts, as presented in figure 23. The strain was therefore used further for introducing the recombinant plasmid containing the post-PKS genes.

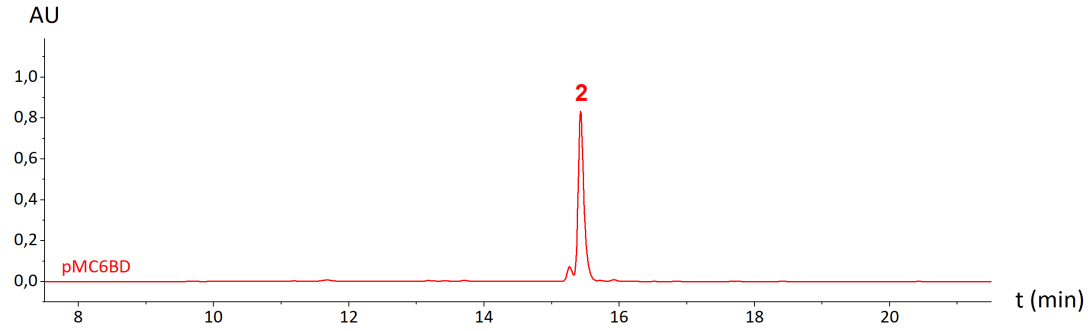

Figure 23. UPLC analysis of the production of UWM6 (2) with the pMC6BD plasmid. The chromatogram is measured at 400 nm.

4.2 Design and assembly of the *lug* biosynthetic gene cluster in *E. coli*

The ordered genetic fragments, or BioBricks, including the promoter, were designed with BioBrick-compatible prefixes and suffixes. The gene fragments also contained an RBS prior to the gene. Based on the mechanism of BioBricks, no protected restriction cut sites remained between the genetic fragments, but instead, flanked the whole operon. This enabled both joining additional genetic material, or changing the plasmid backbone entirely, which was done after an operon was successfully assembled. An example of a complete operon is shown in figure 24.

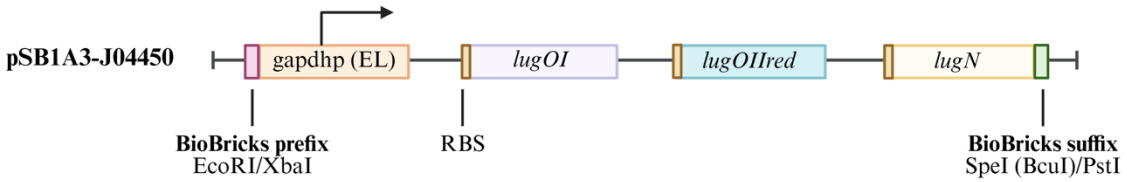

Figure 24. An example of a gene cassette assembled in this study. A plasmid backbone pSB1A3-J04450 was used for the assembly phase. The gene cassette was flanked by a BioBricks compatible prefix and suffix containing recognition sites for digestion. Each gene also contained an RBS sequence prior the gene.

The first-round constructs contained three post-PKS tailoring enzyme genes from the *lug* biosynthetic gene cluster, *lugOI*, *lugOIIred*, and *lugN*. In addition, a landomycin-pathway-derived *lanV* was used to replace its ortholog *lugOIIred* in some constructs to compare their function and activity. Either two or three genes were cloned into an operon

containing a single gapdhp (EL) promoter. The BioBrick-compatible backbone pSB1A3-J04450, with an ampicillin resistance cassette, was used for most constructs in the assembly phase. All the assembled first-round constructs are shown in figure 25.

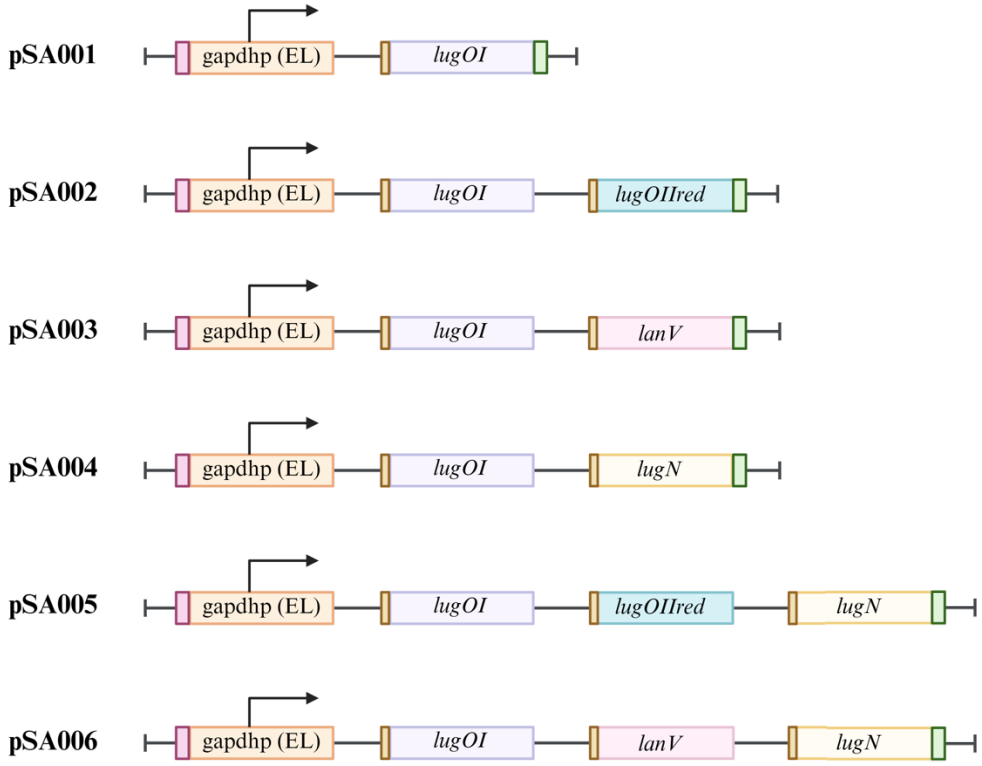

Figure 25. The assembled gene cassettes.

4.3 Heterologous expression of *lug* tailoring genes in *S. coelicolor*

The key intermediate **2** can be further modified into a great variety of products via post-PKS tailoring. The assembled recombinant plasmids containing the post-PKS tailoring genes were introduced into the *S. coelicolor* M1152Δ*matAB* expression strain containing the pMC6BD plasmid for modification of **2** towards **1**. Bacterial conjugation was used to transfer the recombinant plasmids from *E. coli* into the *Streptomyces* host strain. Before transformation into the donor strain, the recombinant operons were ligated into a pSET152-based plasmid, engineered to be BioBricks-compatible. The pSET152BB vector contains an oriT, or origin of transfer, sequence that is essential for successful bacterial conjugation. (Bierman et al. 1992) During conjugation, a single DNA strand is nicked at the oriT site on the plasmid being transferred, and a relaxase enzyme is attached to the 5' end. This complex is then delivered to the recipient cell, where the plasmid is re-circularized. (Pettis 2018).

The *E. coli* ET12567/pUZ8002 strain, to which the recombinant plasmid was transformed after assembly in *E. coli* TOP10, was used as the donor strain for conjugation. *E. coli* ET12567 is a methylation-deficient strain, lacking the methylation markers that could lead to degradation of foreign DNA in either the donor or the recipient strain, making it ideal for conjugation. Additionally, the strain carries a widely used pUZ8002 helper plasmid, which contains the conjugative machinery required for plasmid transfer into *Streptomyces*. (Larcombe et al. 2024).

The heterologous expression strains containing the pMC6BD plasmid for production of UWM6 and plasmids pSA001 to pSA006 containing lugdunomycin tailoring genes in different combinations were cultivated in SG medium for production of angucyclines. Metabolite production was analyzed on UV-Vis UHPLC to ensure the success of the conjugation, and to ensure proper function of the genes (figure 26). The engineered plasmids were expected to catalyze the conversion of the main product of pMC6BD, **2**, into 12-hydroxy-UWM6 (**3**), which is quickly converted into common angucycline metabolites, such as rabelomycin (**4**) and tetrangomycin (**5**). A strain containing pMC6BD and pSA004 plasmids, which encode for genes that function as a branching point towards the C-ring cleavage of **1**, was first cultivated to ensure gene function before conjugating the rest of the strains. An adsorbent LXA1180 resin was used in the main culture to adsorb and preserve metabolites.

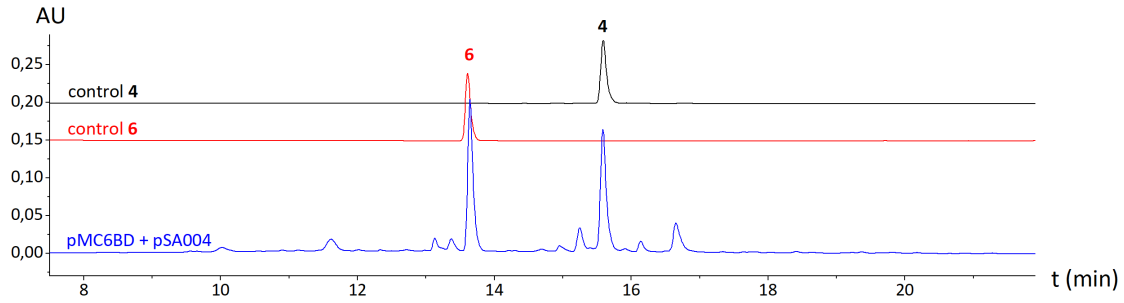

Figure 26. Metabolite production of pMC6BD and pSA004 containing strain. Both rabelomycin (**4**) and methylrabelomycin (**6**) were efficiently produced. The chromatogram is measured at 400 nm.

A high yield of the expected metabolites, **4** and its methylated form, 8-*O*-methylrabelomycin (**6**), was achieved, suggesting the correct function of the engineered constructs. All compounds were identified by comparing their retention times and UV-

Vis spectra to those of control compounds analysed under the same conditions. After ensuring the correct function of the engineered strains, the rest were cultivated in similar conditions.

4.4 Culture condition optimization for angucycline production in *Streptomyces*

When cultivating *Streptomyces*, several strategies were used to optimize and enhance the production of the target metabolites. First, three different medias were evaluated to analyse metabolite production on UHPLC. The *S. coelicolor* host strain with pMC6BD with either pSA002 or pSA006 was grown in E1, MS, and SG medias (figure 27).

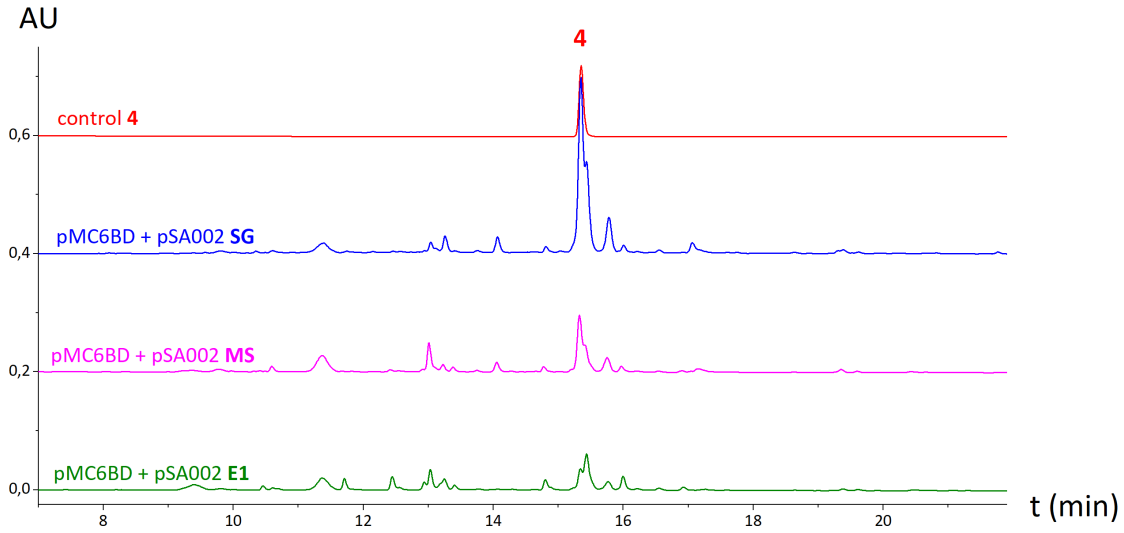

Figure 27. Comparison of the effect of different medias on the production of rabelomycin (4). The chromatogram is measured at 400 nm.

The production profiles showed significant variance between the three medias. Based on elution time and UV-Vis spectra, the peak immediately right from **4** is likely **5**, which was produced by far the most when culturing the strain in SG media. The production of **4** was also noticeably higher compared to the other compounds across all medias. The number of by-products was relatively small in all samples. Similar results could be seen in parallel samples, as well as when culturing other strains in the same conditions.

Other recombinant plasmid containing strains were also used for analysing the effects of different medias. The addition of the *lugN* methyltransferase to form **6** and the methylated product of tetrangomycin, 8-*O*-methyltetrangomycin (**7**) in pSA006 was evaluated with the same three medias as above (figure 28).

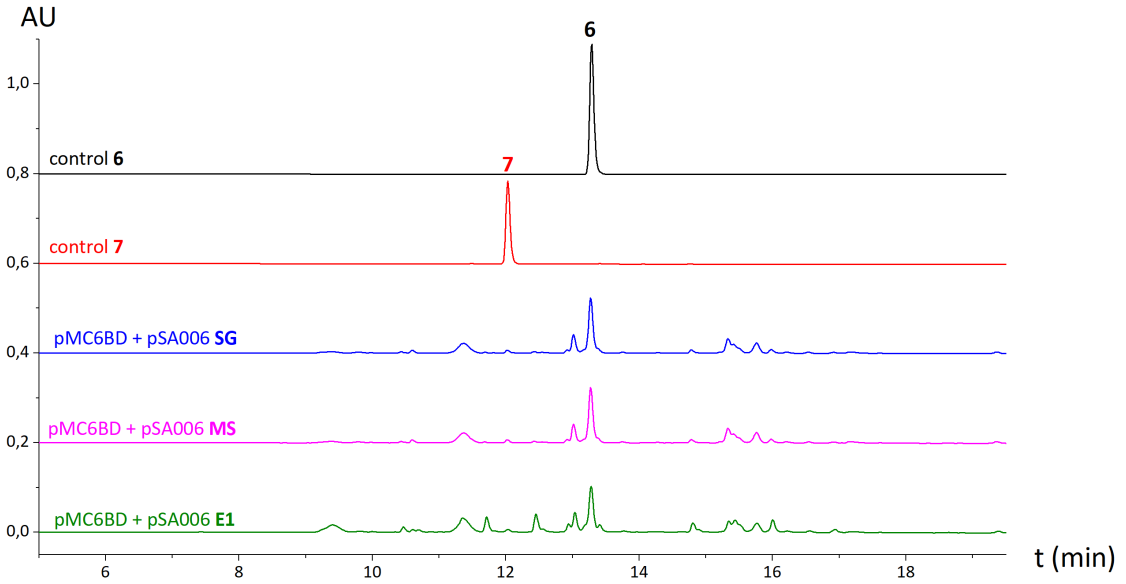

Figure 28. Comparison of the effect of different medias on the production of 8-*O*-methylrabelomycin (6) and 8-*O*-methyltetrangomycin (7). The chromatogram is measured at 400 nm.

Unlike with pSA002, the use of different medias did not greatly affect production after the *lugN* gene was added, as the production profiles between all samples were highly similar in pSA006 containing strains. LugN should lead to the conversion of the early pathway products **4** and **5** into their 8-*O*-methylated forms. A noticeable amount of **6** was produced, which shows *lugN* working as expected. However, the formation of **7** remained poor, as no significant peaks could be identified. LanV functions similarly to its lugdunomycin pathway ortholog LugOIIred by performing the C6 ketoreduction reaction. Despite having an additional function in C1 ketoreduction, LugOIIred is expected to perform similarly to LanV in reducing the product of LugOI (Nuutila et al. 2024). Therefore, LanV and LugN should lead to the formation of **5** and its methylated form **7**, alongside **4** and **6**. Based on these results, SG was used in the following rounds of culturing due to the best yield of target compounds among the three medias.

Due to the low product yields observed across all medias, further optimization steps were taken to enhance the formation of especially the methylated compounds. The addition of the adsorbent LXA1180 resin might have interfered with bacterial growth and metabolite production. The resin is crucial in capturing and stabilizing the metabolites, and protecting them from degradation and unwanted modifications, thereby improving the production of target compounds while minimizing byproduct formation. Cultivating the strains without an adsorbent resulted in accumulation of metabolites, as well as degradation and metabolization of intermediates, leading to formation of undesired

products in large amounts. Thus, to both minimize potential interference with bacterial growth, but also to enable capturing of the target compounds, the resin was added to the cultivations on the third day of culturing the main strains, as opposed to on the first day, as was done previously.

The method of analysis with UV-Vis UHPLC was also improved based on earlier findings. To enhance peak separation for key products, mainly **4** and **5**, in future analyses, the UPLC column was replaced with an alternative column with improved selectivity. To replace the previously used C18 column, the phenyl-hexyl column was chosen due to its ability for improved separation of structurally similar compounds, especially when analysing aromatic compounds.

To evaluate the production of intermediate and target compounds, two time-point samples were taken from two cultures containing either *lugOIIred* or *lanV* in pSA005 and pSA006, respectively. Samples were taken at days 5 and 8 of cultivation of the main cultures, and the results are shown in figure 29.

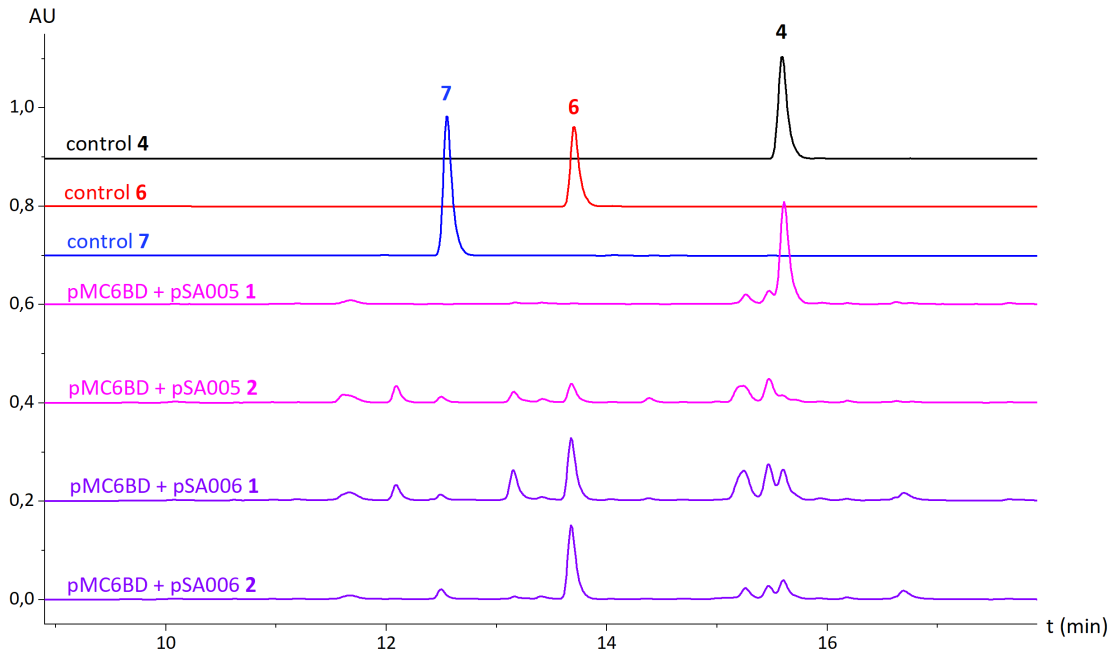

Figure 29. UPLC analysis of production of 4, 6, and 7 at different time points. The chromatogram is measured at 400 nm.

The efficient formation of the early pathway products, mainly **4**, could be seen at day 5, as expected. At day 5, the pSA005 containing strain showed high levels of **4** without by-products in notable amounts. By day 8, **4** was metabolized further resulting in

considerably smaller amounts of various end-products, visualized by multiple small peaks. Compound **6** was formed by day 8, whereas the amount of **4** is significantly lower at a later time point. This is consistent with the presumption of **4** being produced early in the pathway, after which the concentration is decreased due to its metabolization into various end-products. Neither **5** nor its methylated form **7** can, however, be distinguished in notable amounts, thereby again showing poor function of *lugOIIred*. In the strain with pSA006, the difference between the two time points is less visible. Still, the formation of the major metabolites can be seen, with the early products present at larger quantities at day 5, after which their amount decreases slightly likely due to metabolization. In addition, the formation of tetrangomycin by *lanV* seems to be better compared to *lugOIIred*, consistent with earlier results. The most evident example of the efficient function of *lanV* is the formation of **7** in high amount at day 8, when compared to *lugOIIred.*

4.5 Optimization of gene expression levels in *Streptomyces*

Even though the expression studies supported the functional assignment of all the tailoring genes, there was a consistent lack of **5** and **7** throughout the results. Compound **5** is formed via C6 ketoreduction by, for example, LugOIIred or LanV. The yield of **5** and **7** remained poor despite various attempts in improving culturing conditions, therefore suggesting that the activity of the corresponding genes, especially *lugOIIred*, was insufficient. In addition, the first gene in the designed plasmids, *lugOI*, that leads the pathway from **2** to **3**, might be too active compared to the remaining genes. The formation of **4** and its methylation into **6** by LugN represents a shunt pathway, with no further products being formed from either of the shunt pathway intermediates using the current set of genes. However, LugOI is necessary when producing **5** and **7** from **1**. Therefore, new expression constructs were designed to first, increase the activity of the C6 ketoreductase and second, to decrease the activity of the C12 hydroxylase LugOI. The activity of the C6 ketoreductase *lugOIIred* seemed particularly low, and therefore its function was greatly enhanced with a high activity promoter.

The assembled second-round constructs pSA007-009, shown in figure 30 A, were conjugated into the host strain with pMC6BD to improve production levels of wanted products. The desired expression levels were achieved by adding varying promoters with lower or higher activity, depending on the gene. The synthetic promoter sequences were

obtained from Bai et al. 2015 and modified to be BioBricks compatible by flanking the sequence with a BioBricks prefix and suffix. Figure 30 B shows the relative activity of the used promoters compared to a commonly used *kasOp** promoter with a relative activity of 100 %. The *gapdhp (EL)* promoter used in the first-round assemblies has a relative activity of approximately 50 %, whereas the ordered promoters had either a significantly lower or higher activities. Three different low activity promoters, SP5, SP11, and SP15 were used to decrease the high conversion by LugOI towards the shunt pathway, whereas LugOIIred activity was increased significantly with SP44. In addition, proper expression levels were ensured by adding terminator sequences after every gene.

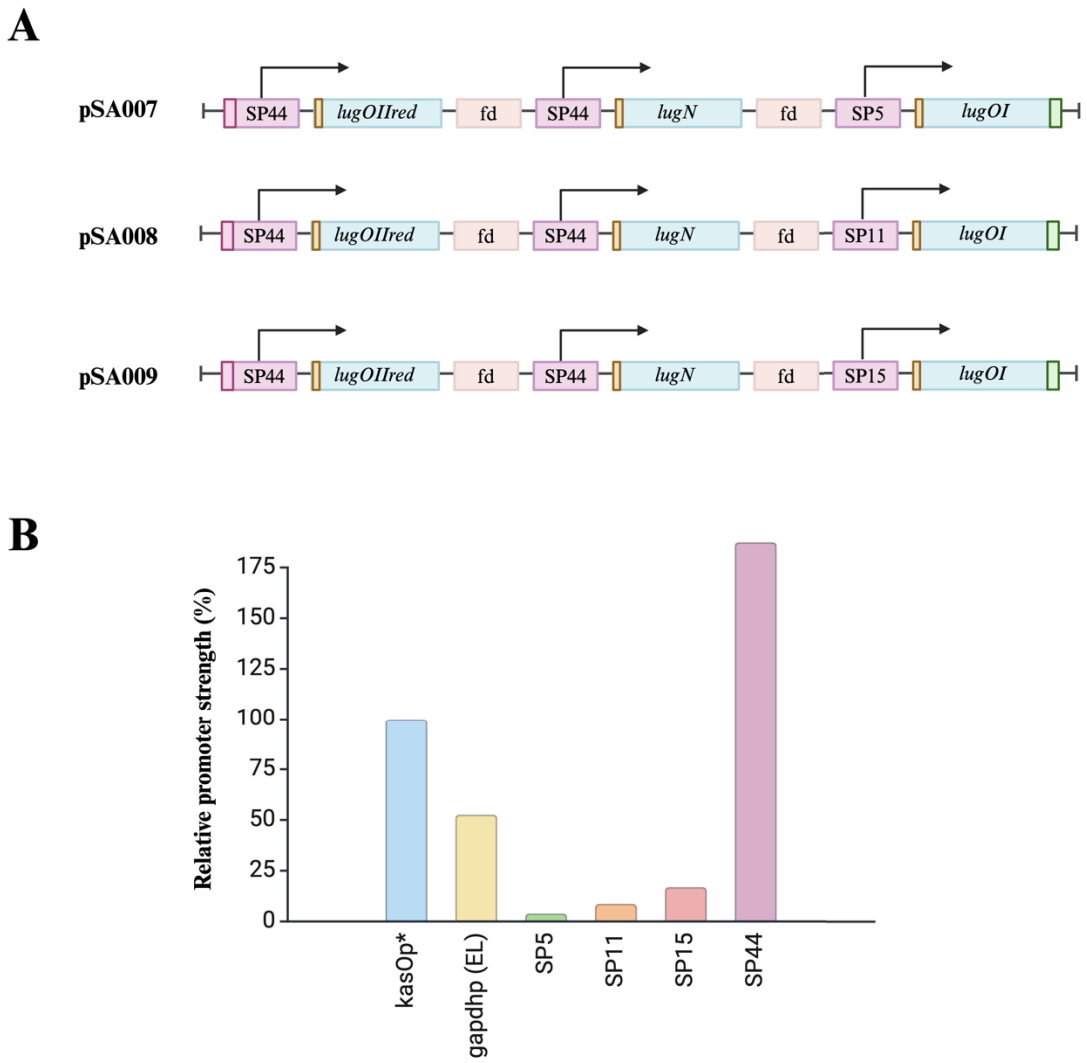

Figure 30. A. The assembled second-round constructs with balanced expression levels. B. The relative strengths of the used promoters in comparison to the widely used kasOp* promoter. (Bai et al. 2015)

4.5.1 Promoter activity analysis with synthetic regulatory elements

Balancing the expression levels of the used genes via synthetic promoters resulted in the pathway being slightly guided away from the shunt product **4**. As opposed to all the first-round strains, a higher yield of **5** compared to **4** was successfully obtained, although the difference in amounts produced was not significant (figure 31). However, the methylated products showed no improvement in production profiles, as the shunt product **6** was again produced in greater quantities when compared to the wanted intermediate **7**, which could not be differentiated from the background peaks. All chromatograms showed a noisy baseline with many background peaks, which further complicates obtaining clear data.

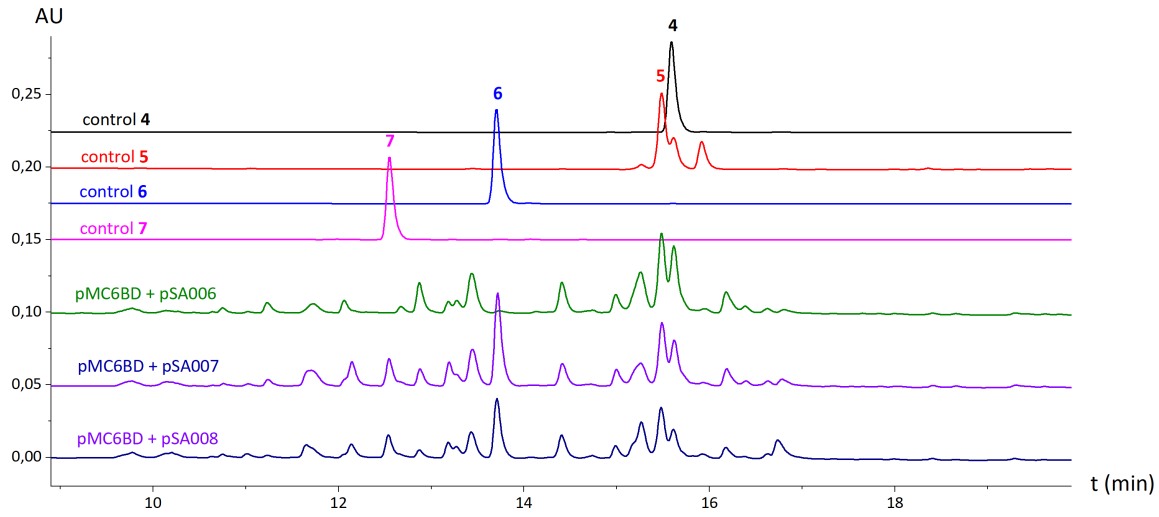

Figure 31. The UPLC analysis of production of compounds 4-7. The chromatogram is measured at 400 nm.

In most cases, the orthologous landomycin pathway enzyme LanV seemed to perform better as a C6 ketoreductase when compared to LugOIIred. The activity and function of both genes was compared by culturing them together in optimized conditions. The data obtained supports earlier findings, as the *lanV* containing construct results in significantly higher yields of **6** with a small peak of **7**, whereas using *lugOIIred* resulted in a smaller peak of **6**, and **7** could not be identified from the chromatogram, as shown in figure 32.

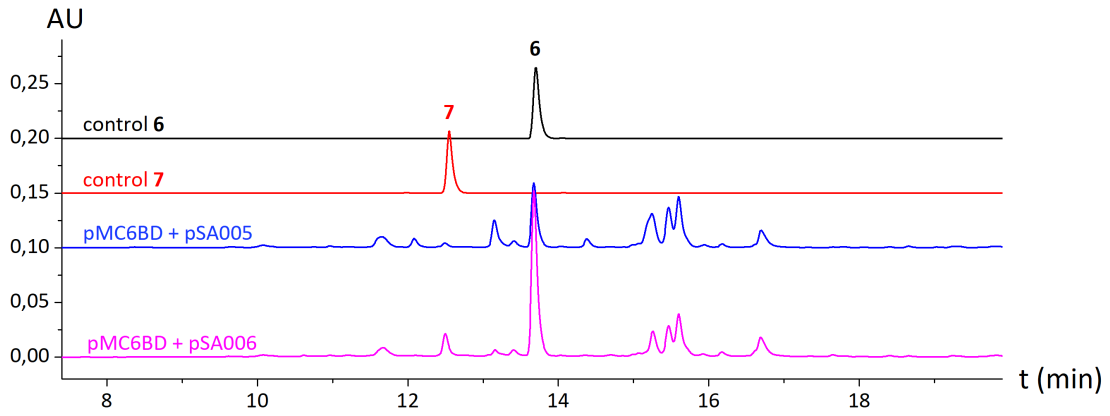

Figure 32. Comparison between *lugOIIred* and *lanV* in production of 6 and 7. The chromatogram is measured at 400 nm.

The improved production with LanV suggests it might outperform the native LugOIIred enzyme in C6 ketoreduction. This can occur due to several reasons, such as substrate specificity, interaction with other enzymes, or a better catalytic efficiency. Furthermore, the LanV protein might be produced more efficiently outside the native host, thus yielding in stronger activity when heterologously expressed.

5 Conclusions

A platform for producing angucycline-pathway intermediates was created in *S. coelicolor*, and known metabolites could be produced and identified. Additionally, a gene library consisting of lugdunomycin pathway genes was successfully obtained. Some metabolites, although mostly shunt products, were purified for further *in vitro* analyses for determination the roles of the enzymes involved. However, the production profiles of most strains remained inconsistent, yielding significant background noise and unwanted metabolites.

Poor production of the expected intermediates was obtained especially among the second-round constructs. This occurred despite all strains being grown under identical conditions, suggesting that environmental factors alone cannot explain the inconsistencies. Instead, these findings highlight the complexity and variability of *Streptomyces* metabolism. Secondary metabolism in these organisms is tightly controlled and generally

downregulated under stressful conditions. Additionally, compound instability, degradation, or host toxicity may have contributed to the poor yields of certain products, such as compounds **5** and **7**. Thus, the poor expression levels are not likely due to environmental factors or transcriptional issues, but rather complex and misunderstood *Streptomyces* metabolism. Moreover, the functional validation of the used plasmids was successful in multiple cases, suggesting that the constructs themselves were operational. This suggests that the challenges observed were less about gene expression or construct failure and more about the metabolic context of the host. Protein folding may also limit product formation, as it is generally unknown whether heterologous proteins fold efficiently in their native hosts, highlighting the need for proteomic studies to confirm proper folding and activity.

Many angucycline-producing pathways are known to branch out to produce large libraries of compounds, rather than single products on linear pathways (Nuutila et al. 2024) (Nuutila et al. 2024). The phenomenon likely arises from both highly promiscuous tailoring enzymes and others with more substrate specific requirements being present within the same pathways. This leads to the formation of numerous shunt products that complicate both compound detection and analysis. Therefore, the observed products might not be biosynthetic noise, but rather compounds carrying yet undiscovered biological functions or metabolites that might require synergistic function to reach bioactivity.

In bacterial expression systems, such as the ones used in this study, a wide variety of components can be optimized from the genetic parts themselves to many variables in the culture conditions. Furthermore, the more complex the organism is, the more there generally is to learn and optimize. At the scale of bacterial organisms, the metabolic network of *Streptomyces* is highly intricate, as well as poorly understood. Balancing a variety of complex pathway genes is crucial for precise expression of specific metabolites, which often remains a challenge within *Streptomyces* metabolism. Expressing the biosynthesis of unknown pathways in *Streptomyces* often require significant fine-tuning and multiple cycles of DBTL, and even small changes in host background or expression could lead to major differences in metabolite output. Additionally, more precise synthetic biology tools are needed to facilitate balancing these gene expression levels.

Importantly, this study highlights the importance of experimental validation though *in vivo* expression systems, as the functional characterization cannot rely solely on sequence homology. Heterologous *in vivo* assay systems provide a great way to identify the functional differences of related enzymes, as well as to expand our understanding of the plasticity of angucycline tailoring pathways. Although similar functions, a related enzyme might lead to better efficacy when expressed outside its native host. The precise function of an enzyme and its substrate specificity, as well as possible latent enzyme activities suppressed in native hosts, may also be studied by expressing their corresponding genes from different angucycline gene clusters in a heterologous host.

Lugdunomycin is an intriguing example of the untapped potential for novel metabolite discovery in Actinomycetes such as *Streptomyces*. Since its recent discovery, it has rapidly become recognized due to its unprecedented structure and promising bioactivity. Lugdunomycin and its structural variants may expand the known diversity of polyketides, offering new directions for the ongoing biosynthetic and pharmaceutical research. (Wu et al. 2019) Furthermore, numerous cryptic BGCs with unknown metabolites remain hidden in *Streptomyces* genomes highlighting the capacity for new compound discovery (Palmu et al. 2007). These advances not only renew interest in understudied compounds classes such as non-classical angucyclines but also highlight their value as leads in the development of novel antimicrobial agents.

6 References

Aigle, B., Lautru, S., Spiteller, D., Dickschat, J. S., Challis, G. L., Leblond, P. & Pernodet, J.-L. (2014) Genome mining of *Streptomyces ambofaciens*. *Journal of Industrial Microbiology and Biotechnology* **41**:251–263.

Akiyama, T., Harada, S., Kojima, F., Takahashi, Y., Imada, C., Okami, Y., … Takeuchi, T. (1998) Fluostatins A and B, New Inhibitors of Dipeptidyl Peptidase III, Produced by Streptomyces sp. TA-3391. I. Taxonomy of Producing Strain, Production, Isolation, Physico-chemical Properties and Biological Properties. *J Antibiot* **51**:553–559.

Albarano, L., Esposito, R., Ruocco, N. & Costantini, M. (2020) Genome Mining as New Challenge in Natural Products Discovery. *Mar Drugs* **18**:199.

Antoraz, S., Santamaría, R. I., Díaz, M., Sanz, D. & Rodríguez, H. (2015) Toward a new focus in antibiotic and drug discovery from the Streptomyces arsenal. *Front Microbiol* **6**:461.

Årdal, C., Balasegaram, M., Laxminarayan, R., McAdams, D., Outterson, K., Rex, J. H. & Sumpradit, N. (2020) Antibiotic development—Economic, regulatory and societal challenges. *Nat Rev Microbiol* **18**:267–274.

Bai, C., Zhang, Y., Zhao, X., Hu, Y., Xiang, S., Miao, J., … Zhang, L. (2015) Exploiting a precise design of universal synthetic modular regulatory elements to unlock the microbial natural products in *Streptomyces*. *Proc Natl Acad Sci USA* **112**:12181–12186.

Balitz, D. M., O''Herron, F. A., Bush, J., Vyas, D. M., Nettleton, D. E., Grulich, R. E., … Clardy, J. (1981) Antitumor agents from Streptomyces anandii: Gilvocarcins V, M and E. *J Antibiot* **34**:1544–1555.

Baltz, R. H. (2016) Genetic manipulation of secondary metabolite biosynthesis for improved production in *Streptomyces* and other actinomycetes. *Journal of Industrial Microbiology and Biotechnology* **43**:343–370.

Beyer, P. & Paulin, S. (2020) The Antibacterial Research and Development Pipeline Needs Urgent Solutions. *ACS Infect Dis* **6**:1289–1291.

Bibb, M. J. (2005) Regulation of secondary metabolism in streptomycetes. *Current Opinion in Microbiology* **8**:208–215.

Bierman, M., Logan, R., O'Brien, K., Seno, E. T., Nagaraja Rao, R. & Schoner, B. E. (1992) Plasmid cloning vectors for the conjugal transfer of DNA from Escherichia coli to Streptomyces spp. *Gene* **116**:43–49.

Bunet, R., Song, L., Mendes, M. V., Corre, C., Hotel, L., Rouhier, N., … Aigle, B. (2011) Characterization and Manipulation of the Pathway-Specific Late Regulator AlpW Reveals *Streptomyces ambofaciens* as a New Producer of Kinamycins. *J Bacteriol* **193**:1142–1153.

Bush, K., Courvalin, P., Dantas, G., Davies, J., Eisenstein, B., Huovinen, P., … Zgurskaya, H. I. (2011) Tackling antibiotic resistance. *Nat Rev Microbiol* **9**:894–896.

Chen, Y., Fan, K., He, Y., Xu, X., Peng, Y., Yu, T., … Yang, K. (2010) Characterization of JadH as an FAD- and NAD(P)H-Dependent Bifunctional Hydroxylase/Dehydrase in Jadomycin Biosynthesis. *ChemBioChem* **11**:1055–1060.

Chen, Y.-H., Wang, C.-C., Greenwell, L., Rix, U., Hoffmeister, D., Vining, L. C., … Yang, K.-Q. (2005) Functional Analyses of Oxygenases in Jadomycin Biosynthesis and Identification of JadH as a Bifunctional Oxygenase/Dehydrase. *Journal of Biological Chemistry* **280**:22508–22514.

Christaki, E., Marcou, M. & Tofarides, A. (2020) Antimicrobial Resistance in Bacteria: Mechanisms, Evolution, and Persistence. *J Mol Evol* **88**:26–40.

Cibichakravarthy, B. & Jose, P. A. (2021) Biosynthetic Potential of Streptomyces Rationalizes Genome-Based Bioprospecting. *Antibiotics* **10**:873.

De Lima Procópio, R. E., Da Silva, I. R., Martins, M. K., De Azevedo, J. L. & De Araújo, J. M. (2012) Antibiotics produced by Streptomyces. *The Brazilian Journal of Infectious Diseases* **16**:466–471.

Drautz, H., Zähner, H., Rohr, J. & Zeeck, A. (1986) Metabolic products of microorganisms. 234 Urdamycins, new angucycline antibiotics from Streptomyces fradiae. I Isolation, characterization and biological properties. *J Antibiot* **39**:1657–1669.

Durand, G. A., Raoult, D. & Dubourg, G. (2019) Antibiotic discovery: History, methods and perspectives. *Int J Antimicrob Agents* **53**:371–382.

Elsayed, S. S., Van Der Heul, H. U., Xiao, X., Nuutila, A., Baars, L. R., Wu, C., … Van Wezel, G. P. (2023) Unravelling key enzymatic steps in C-ring cleavage during angucycline biosynthesis. *Commun Chem* **6**:281.

European Centre for Disease Prevention and Control. (2018) *Surveillance of antimicrobial resistance in Europe: Annual report of the European Antimicrobial Resistance Surveillance Network (EARS Net) 2017.* LU: Publications Office. Retrieved from https://data.europa.eu/doi/10.2900/230516

Fan, K., Pan, G., Peng, X., Zheng, J., Gao, W., Wang, J., … Yang, K. (2012) Identification of JadG as the B Ring Opening Oxygenase Catalyzing the Oxidative C-C Bond Cleavage Reaction in Jadomycin Biosynthesis. *Chemistry & Biology* **19**:1381–1390.

Fan, K. & Zhang, Q. (2018) The functional differentiation of the post-PKS tailoring oxygenases contributed to the chemical diversities of atypical angucyclines. *Synthetic and Systems Biotechnology* **3**:275–282.

Faust, B., Hoffmeister, D., Weitnauer, G., Westrich, L., Haag, S., Schneider, P., … Bechthold, A. (2000) Two new tailoring enzymes, a glycosyltransferase and an oxygenase, involved in biosynthesis of the angucycline antibiotic urdamycin A in Streptomyces fradiae Tü2717 This paper is dedicated to Professor Heinz Floss, a pioneer in the field of antibiotics, on the occasion of his 65th birthday. The GenBank accession numbers for the sequences reported in this paper are AF164960 and AF164961. *Microbiology* **146**:147–154.

G8 Science Ministers Statement, London UK, 12 June 2013 (2013, June 13). Department for Business, Innovation & Skills (UK Government). Retrieved from https://www.gov.uk/government/publications/g8-science-ministers-statement-london-12-june-2013

Genilloud, O. (2019) Natural products discovery and potential for new antibiotics. *Current Opinion in Microbiology* **51**:81–87.

Gould, S. J., Hong, S.-T. & Carney, J. R. (1998) Cloning and Heterologous Expression of Genes from the Kinamycin Biosynthetic Pathway of Streptomyces murayamaensis. *J Antibiot* **51**:50–57.

Guo, F., Xiang, S., Li, L., Wang, B., Rajasärkkä, J., Gröndahl-Yli-Hannuksela, K., … Yang, K. (2015) Targeted activation of silent natural product biosynthesis pathways by reporter-guided mutant selection. *Metabolic Engineering* **28**:134–142.

Hasinoff, B. B., Wu, X., Yalowich, J. C., Goodfellow, V., Laufer, R. S., Adedayo, O. & Dmitrienko, G. I. (2006) Kinamycins A and C, bacterial metabolites that contain an unusual diazo group, as potential new anticancer agents: Antiproliferative and cell cycle effects. *Anti-Cancer Drugs* **17**:825–837.

Henkel, T., Rohr, J., Beale, J. M. & Schwenen, L. (1990) Landomycins, new angucycline antibiotics from Streptomyces sp. I. Structural studies on landomycins A-D. *J Antibiot* **43**:492–503.

Hertweck, C. (2009) The Biosynthetic Logic of Polyketide Diversity. *Angew Chem Int Ed* **48**:4688–4716.

Hertweck, C., Luzhetskyy, A., Rebets, Y. & Bechthold, A. (2007) Type II polyketide synthases: Gaining a deeper insight into enzymatic teamwork. *Nat Prod Rep* **24**:162–190.

Huang, C., Yang, C., Zhang, W., Zhang, L., De, B. C., Zhu, Y., … Zhang, C. (2018) Molecular basis of dimer formation during the biosynthesis of benzofluorene-containing atypical angucyclines. *Nat Commun* **9**:2088.

Ito, S., Matsuya, T., Omura, S., Otani, M., Nakagawa, A., Takeshima, H., … Hata, T. (1970) A NEW ANTIBIOTIC, KINAMYCIN. *J Antibiot* **23**:315–317.

Jin, J., Yang, X., Liu, T., Xiao, H., Wang, G., Zhou, M., … Ma, M. (2018) Fluostatins M-Q Featuring a 6-5-6-6 Ring Skeleton and High Oxidized A-Rings from Marine Streptomyces sp. PKU-MA00045. *Mar Drugs* **16**:87.

Jones, S. E. & Elliot, M. A. (2017) Streptomyces Exploration: Competition, Volatile Communication and New Bacterial Behaviours. *Trends in Microbiology* **25**:522–531.

Kallio, P., Liu, Z., Mäntsälä, P., Niemi, J. & Metsä-Ketelä, M. (2008) Sequential Action of Two Flavoenzymes, PgaE and PgaM, in Angucycline Biosynthesis: Chemoenzymatic Synthesis of Gaudimycin C. *Chemistry & Biology* **15**:157–166.

Kallio, P., Patrikainen, P., Suomela, J.-P., Mäntsälä, P., Metsä-Ketelä, M. & Niemi, J. (2011) Flavoprotein Hydroxylase PgaE Catalyzes Two Consecutive Oxygen-Dependent Tailoring Reactions in Angucycline Biosynthesis. *Biochemistry* **50**:5535–5543.

Kersten, R. D., Lane, A. L., Nett, M., Richter, T. K. S., Duggan, B. M., Dorrestein, P. C. & Moore, B. S. (2013) Bioactivity-guided genome mining reveals the lomaiviticin biosynthetic gene cluster in Salinispora tropica. *Chembiochem* **14**:955–962.

Kharel, M. K., Pahari, P., Shaaban, K. A., Wang, G., Morris, C. & Rohr, J. (2012) Elucidation of post-PKS tailoring steps involved in landomycin biosynthesis. *Org Biomol Chem* **10**:4256.

Kharel, M. K., Pahari, P., Shepherd, M. D., Tibrewal, N., Nybo, S. E., Shaaban, K. A. & Rohr, J. (2012) Angucyclines: Biosynthesis, mode-of-action, new natural products, and synthesis. *Nat Prod Rep* **29**:264–325.

Kharel, M. K. & Rohr, J. (2012) Delineation of gilvocarcin, jadomycin, and landomycin pathways through combinatorial biosynthetic enzymology. *Curr Opin Chem Biol* **16**:150–161.

Kharel, M. K., Zhu, L., Liu, T. & Rohr, J. (2007) Multi-oxygenase complexes of the gilvocarcin and jadomycin biosyntheses. *J Am Chem Soc* **129**:3780–3781.

Knight, Tom (2003) *Idempotent vector design for standard assembly of BioBricks*. Cambridge, MA: MIT Synthetic Biology Working Group. Retrieved from http://hdl.handle.net/1721.1/21168

Knight, Tom *Idempotent vector design for standard assembly of BioBricks* [Data set].

Komaki, H. (2023) Recent Progress of Reclassification of the Genus Streptomyces. *Microorganisms* **11**:831.

Lacey, H. J. & Rutledge, P. J. (2022) Recently Discovered Secondary Metabolites from Streptomyces Species. *Molecules* **27**:887.

Larcombe, D. E., Braes, R. E., Croxford, J. T., Wilson, J. W., Figurski, D. H. & Hoskisson, P. A. (2024) Sequence and origin of the Streptomyces intergenetic-conjugation helper plasmid pUZ8002. *Access Microbiology* **6**.

Li, Z., Zhu, D. & Shen, Y. (2018) Discovery of novel bioactive natural products driven by genome mining. *DD&T* **12**:318–328.

Liu, H.-S., Chen, H.-R., Huang, S.-S., Li, Z.-H., Wang, C.-Y. & Zhang, H. (2025) Bioactive Angucyclines/Angucyclinones Discovered from 1965 to 2023. *Marine Drugs* **23**:25.

Liu, T., Kharel, M. K., Fischer, C., McCormick, A. & Rohr, J. (2006) Inactivation of gilGT, encoding a C-glycosyltransferase, and gilOIII, encoding a P450 enzyme, allows the details of the late biosynthetic pathway to gilvocarcin V to be delineated. *Chembiochem* **7**:1070–1077.

Liu, X., Liu, D., Xu, M., Tao, M., Bai, L., Deng, Z., … Jiang, M. (2018a) Reconstitution of Kinamycin Biosynthesis within the Heterologous Host *Streptomyces albus* J1074. *J Nat Prod* **81**:72–77.

Luzhetskyy, A., Vente, A. & Bechthold, A. (2005) Glycosyltransferases involved in the biosynthesis of biologically active natural products that contain oligosaccharides. *Mol BioSyst* **1**:117.

Ma, M., Rateb, M. E., Teng, Q., Yang, D., Rudolf, J. D., Zhu, X., … Shen, B. (2015) Angucyclines and Angucyclinones from *Streptomyces* sp. CB01913 Featuring C-Ring Cleavage and Expansion. *J Nat Prod* **78**:2471–2480.

Malico, A. A., Nichols, L. & Williams, G. J. (2020) Synthetic biology enabling access to designer polyketides. *Current Opinion in Chemical Biology* **58**:45–53.

Mayer, A., Taguchi, T., Linnenbrink, A., Hofmann, C., Luzhetskyy, A. & Bechthold, A. (2005) LanV, a Bifunctional Enzyme: Aromatase and Ketoreductase during Landomycin A Biosynthesis. *ChemBioChem* **6**:2312–2315.

Miethke, M., Pieroni, M., Weber, T., Brönstrup, M., Hammann, P., Halby, L., … Müller, R. (2021) Towards the sustainable discovery and development of new antibiotics. *Nat Rev Chem* **5**:726–749.

Mikhaylov, A. A., Ikonnikova, V. A. & Solyev, P. N. (2021) Disclosing biosynthetic connections and functions of atypical angucyclinones with a fragmented C-ring. *Nat Prod Rep* **38**:1506–1517.

Morrison, L. & Zembower, T. R. (2020) Antimicrobial Resistance. *Gastrointestinal Endoscopy Clinics of North America* **30**:619–635.

Navarro-Muñoz, J. C., Selem-Mojica, N., Mullowney, M. W., Kautsar, S. A., Tryon, J. H., Parkinson, E. I., … Medema, M. H. (2020) A computational framework to explore large-scale biosynthetic diversity. *Nat Chem Biol* **16**:60–68.

Nguyen, C. T., Dhakal, D., Pham, V. T. T., Nguyen, H. T. & Sohng, J.-K. (2020) Recent Advances in Strategies for Activation and Discovery/Characterization of Cryptic Biosynthetic Gene Clusters in Streptomyces. *Microorganisms* **8**:616.

Nivina, A., Yuet, K. P., Hsu, J. & Khosla, C. (2019) Evolution and Diversity of Assembly-Line Polyketide Synthases. *Chem Rev* **119**:12524–12547.

Nuutila, A., Xiao, X., Van Der Heul, H. U., Van Wezel, G. P., Dinis, P., Elsayed, S. S. & Metsä-Ketelä, M. (2024) Divergence of Classical and C-Ring-Cleaved Angucyclines: Elucidation of Early Tailoring Steps in Lugdunomycin and Thioangucycline Biosynthesis. *ACS Chem Biol* **19**:1131–1141.

Olano, C., Méndez, C. & Salas, J. A. (2010) Post-PKS tailoring steps in natural product-producing actinomycetes from the perspective of combinatorial biosynthesis. *Nat Prod Rep* **27**:571.

Paananen, P., Patrikainen, P., Kallio, P., Mäntsälä, P., Niemi, J., Niiranen, L. & Metsä-Ketelä, M. (2013) Structural and Functional Analysis of Angucycline C-6 Ketoreductase LanV Involved in Landomycin Biosynthesis. *Biochemistry* **52**:5304–5314.

Pahari, P., Kharel, M. K., Shepherd, M. D., van Lanen, S. G. & Rohr, J. (2012) Enzymatic total synthesis of defucogilvocarcin M and its implications for gilvocarcin biosynthesis. *Angew Chem Int Ed Engl* **51**:1216–1220.

Pahari, P., Kharel, M. K., Shepherd, M. D., van Lanen, S. G. & Rohr, J. (2012) Enzymatic Total Synthesis of Defucogilvocarcin M and Its Implications for Gilvocarcin Biosynthesis. *Angew Chem Int Ed* **51**:1216–1220.

Palmu, K., Ishida, K., Mäntsälä, P., Hertweck, C. & Metsä-Ketelä, M. (2007) Artificial Reconstruction of Two Cryptic Angucycline Antibiotic Biosynthetic Pathways. *ChemBioChem* **8**:1577–1584.

Pan, G., Gao, X., Fan, K., Liu, J., Meng, B., Gao, J., … Yang, K. (2017) Structure and Function of a C–C Bond Cleaving Oxygenase in Atypical Angucycline Biosynthesis. *ACS Chem Biol* **12**:142–152.

Patrikainen, P., Kallio, P., Fan, K., Klika, K. D., Shaaban, K. A., Mäntsälä, P., … Metsä-Ketelä, M. (2012) Tailoring Enzymes Involved in the Biosynthesis of Angucyclines Contain Latent Context-Dependent Catalytic Activities. *Chemistry & Biology* **19**:647–655.

Pettis, G. S. (2018) Spreading the news about the novel conjugation mechanism in *Streptomyces* bacteria. *Environ Microbiol Rep* **10**:503–510.

Risdian, C., Mozef, T. & Wink, J. (2019) Biosynthesis of Polyketides in Streptomyces. *Microorganisms* **7**:124.

Rivers, M. A. J. & Lowell, A. N. (2024) Expanding the Biosynthetic Toolbox: The Potential and Challenges of In Vitro Type II Polyketide Synthase Research. *SynBio* **2**:85–111.

Rix, U., Remsing, L. L., Hoffmeister, D., Bechthold, A. & Rohr, J. (2003) Urdamycin L: A Novel Metabolic Shunt Product that Provides Evidence for the Role of the *urd* M Gene in the Urdamycin A Biosynthetic Pathway of *Streptomyces fradiae* TÜ 2717. *ChemBioChem* **4**:109–111.

Rix, U., Wang, C., Chen, Y., Lipata, F. M., Remsing Rix, L. L., Greenwell, L. M., … Rohr, J. (2005) The Oxidative Ring Cleavage in Jadomycin Biosynthesis: A Multistep Oxygenation Cascade in a Biosynthetic Black Box. *ChemBioChem* **6**:838–845.

Rix, U., Zheng, J., Remsing Rix, L. L., Greenwell, L., Yang, K. & Rohr, J. (2004) The Dynamic Structure of Jadomycin B and the Amino Acid Incorporation Step of Its Biosynthesis. *J Am Chem Soc* **126**:4496–4497.

Rohr, J. (1989) Urdamycins, new angucycline antibiotics from Streptomyces fradiae. VI. Structure elucidation and biosynthetic investigations on urdamycin H. *J Antibiot* **42**:1482–1488.

Rohr, J., Beale, J. M. & Floss, H. G. (1989) Urdamycins, new angucycline antibiotics from Streptomyces fradiae. IV. Biosynthetic studies of urdamycins A-D. *J Antibiot* **42**:1151–1157.

Rohr, J. & Zeeck, A. (1987) Metabolic products of microorganisms. 240 Urdamycins, new angucycline antibiotics from Streptomyces fradiae. II Structural studies of urdamycins B to F. *J Antibiot* **40**:459–467.

Shetty, R., Lizarazo, M., Rettberg, R. & Knight, T. F. (2011) Assembly of BioBrick Standard Biological Parts Using Three Antibiotic Assembly. In *Methods in Enzymology* (Vol. 498, pp. 311–326). Elsevier.

Shetty, R. P., Endy, D. & Knight, T. F. (2008) Engineering BioBrick vectors from BioBrick parts. *J Biol Eng* **2**:5.

Smith, S. & Tsai, S.-C. (2007) The type I fatty acid and polyketide synthases: A tale of two megasynthases. *Nat Prod Rep* **24**:1041.

Tibrewal, N., Pahari, P., Wang, G., Kharel, M. K., Morris, C., Downey, T., … Rohr, J. (2012) Baeyer-Villiger C-C bond cleavage reaction in gilvocarcin and jadomycin biosynthesis. *J Am Chem Soc* **134**:18181–18184.

Tohyama, S., Nukui, S., Hatano, M., Hayashi, C., Momose, I. & Igarashi, M. (2025) Study about fluostatins: Efficient preparation of fluostatin A and discovery of fluostatin derivatives from Streptomyces sp. TA-3391. *J Antibiot*.

Tolmie, C., Smit, M. S. & Opperman, D. J. (2019) Native roles of Baeyer–Villiger monooxygenases in the microbial metabolism of natural compounds. *Nat Prod Rep* **36**:326–353.

Van Der Meij, A., Worsley, S. F., Hutchings, M. I. & Van Wezel, G. P. (2017) Chemical ecology of antibiotic production by actinomycetes. *FEMS Microbiology Reviews* **41**:392–416.

Vysloužilová, D. & Kováč, O. (2024) The Chemistry of Angucyclines. *ChemPlusChem* **89**:e202400307.

Wang, B., Ren, J., Li, L., Guo, F., Pan, G., Ai, G., … Yang, K. (2015) Kinamycin biosynthesis employs a conserved pair of oxidases for B-ring contraction. *Chem Commun* **51**:8845–8848.

Wang, Jia, Zhang, R., Chen, X., Sun, X., Yan, Y., Shen, X. & Yuan, Q. (2020) Biosynthesis of aromatic polyketides in microorganisms using type II polyketide synthases. *Microb Cell Fact* **19**:110.

Wang, Junyang, Nielsen, J. & Liu, Z. (2021) Synthetic Biology Advanced Natural Product Discovery. *Metabolites* **11**:785.

Wang, R., Nguyen, J., Hecht, J., Schwartz, N., Brown, K. V., Ponomareva, L. V., … Nybo, S. E. (2022) A BioBricks Metabolic Engineering Platform for the Biosynthesis of Anthracyclinones in *Streptomyces coelicolor*. *ACS Synth Biol* **11**:4193–4209.

Watve, M., Tickoo, R., Jog, M. & Bhole, B. (2001) How many antibiotics are produced by the genus Streptomyces ? *Archives of Microbiology* **176**:386–390.

World Health Organization (2024, March 4) Antimicrobial resistance. Retrieved from https://www.who.int/news-room/fact-sheets/detail/antimicrobial-resistance

Wu, C., van der Heul, H. U., Melnik, A. V., Lübben, J., Dorrestein, P. C., Minnaard, A. J., … van Wezel, G. P. (2019) Lugdunomycin, an Angucycline-Derived Molecule with Unprecedented Chemical Architecture. *Angew Chem Int Ed* **58**:2809–2814.

Xiao, X., Elsayed, S. S., Wu, C., Van Der Heul, H. U., Metsä-Ketelä, M., Du, C., … Van Wezel, G. P. (2020) Functional and Structural Insights into a Novel Promiscuous Ketoreductase of the Lugdunomycin Biosynthetic Pathway. *ACS Chem Biol* **15**:2529–2538.

Xie, S. & Zhang, L. (2023) Type II Polyketide Synthases: A Bioinformatics-Driven Approach. *ChemBioChem* **24**:e202200775.

Xu, X., Huang, X. & Xu, W. (2025a) Marine actinomycetes-derived angucyclines and angucyclinones with biosynthesis and activity—Past 10 years (2014–2023). *European Journal of Medicinal Chemistry* **283**:117161.

Yang, C., Huang, C., Fang, C., Zhang, L., Chen, S., Zhang, Q., … Zhang, W. (2021) Inactivation of Flavoenzyme-Encoding Gene *flsO1* in Fluostatin Biosynthesis Leads to Diversified Angucyclinone Derivatives. *J Org Chem* **86**:11019–11028.

Yang, C., Huang, C., Zhang, W., Zhu, Y. & Zhang, C. (2015) Heterologous Expression of Fluostatin Gene Cluster Leads to a Bioactive Heterodimer. *Org Lett* **17**:5324–5327.

Yang, K., Han, L., Ayer, S. W. & Vining, L. C. (1996) Accumulation of the angucycline antibiotic rabelomycin after disruption of an oxygenase gene in the jadomycin B biosynthetic gene cluster of Streptomyces venezuelae. *Microbiology* **142**:123–132.

Yang, X., Fu, B. & Yu, B. (2011) Total Synthesis of Landomycin A, a Potent Antitumor Angucycline Antibiotic. *J Am Chem Soc* **133**:12433–12435.

Yook, G., Nam, J., Jo, Y., Yoon, H. & Yang, D. (2025) Metabolic engineering approaches for the biosynthesis of antibiotics. *Microb Cell Fact* **24**:35.

Yushchuk, O., Kharel, M., Ostash, I. & Ostash, B. (2019) Landomycin biosynthesis and its regulation in Streptomyces. *Appl Microbiol Biotechnol* **103**:1659–1665.

Zhang, L., Zhao, T., Geng, L., Zhang, C., Xiang, W., Zhang, J., … Shu, C. (2024) Characterization and evaluation of actinomycete from the Protaetia brevitarsis Larva Frass. *Front Microbiol* **15**:1385734.

Zhu, L., Ostash, B., Rix, U., Nur-E-Alam, M., Mayers, A., Luzhetskyy, A., … Rohr, J. (2005) Identification of the function of gene lndM2 encoding a bifunctional oxygenase-reductase involved in the biosynthesis of the antitumor antibiotic landomycin E by Streptomyces globisporus 1912 supports the originally assigned structure for landomycinone. *J Org Chem* **70**:631–638.